



CHALMERS
UNIVERSITY OF TECHNOLOGY

Prospects of Alkali Metal-Se Batteries and Beyond: From Redox Mechanisms to Electrode Design

Downloaded from: <https://research.chalmers.se>, 2025-05-12 17:42 UTC

Citation for the original published paper (version of record):

Park, J., Kim, H., Celeste, A. et al (2025). Prospects of Alkali Metal-Se Batteries and Beyond: From Redox Mechanisms to Electrode Design. ACS Energy Letters, In Press: 2512-2531.
<http://dx.doi.org/10.1021/acsenergylett.5c00768>

N.B. When citing this work, cite the original published paper.

Prospects of Alkali Metal–Se Batteries and Beyond: From Redox Mechanisms to Electrode Design

Jimin Park,[#] Hyerim Kim,[#] Arcangelo Celeste,[#] Hyeona Park, Shivam Kansara, Rosaceleste Zumpano, Vanessa Piacentini, Sergio Brutti, Aleksandar Matic, Marco Agostini,* and Jang-Yeon Hwang*



Cite This: *ACS Energy Lett.* 2025, 10, 2512–2531



Read Online

ACCESS |



Metrics & More

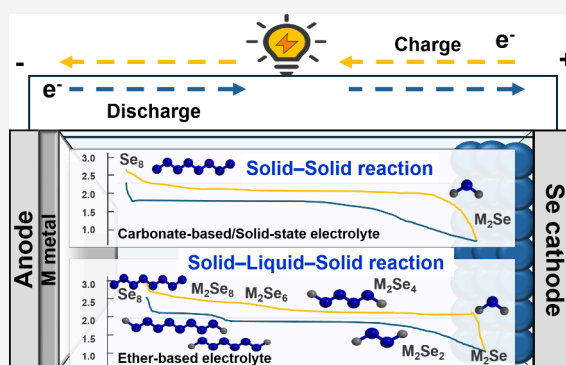


Article Recommendations



Supporting Information

ABSTRACT: Selenium-based alkali metal systems offer significant potential for surpassing commercial Li-ion systems in volumetric energy density (3,253 vs 1,000 mAh cm⁻³). However, challenges remain in electrode design, solid electrolyte interface stability, and mitigating active material dissolution. This review explores redox mechanisms, electrode architectures, and electrolyte strategies for enhancing performance, with a focus on Li, Na, K anodes and beyond. Advances in computational and experimental studies are discussed, highlighting key issues and future research directions to address scalability and improve stability, making Se-based batteries promising candidates for sustainable energy storage.



Modern energy consumption continues to drive the search for innovative and sustainable energy storage solutions. As traditional fossil fuels face increasing scrutiny owing to environmental concerns and finite reserves, the urgency to adopt clean and efficient alternatives has never been more apparent.¹ Renewable energy sources hold significant potential for revolutionizing the energy market. However, clean sources like solar and wind are intermittent and require storage systems to redistribute energy on demand.² Li-ion batteries have historically dominated the energy storage market for portable electronics and electric vehicles, owing to their high energy densities. However, the limited availability of Li and related electrode components has prompted the exploration of alternative chemistries. The scarcity and geographical concentration of Li sources, coupled with rising demand, are expected to increase prices and create geopolitical challenges.³ Selenium-based alkali metal batteries, incorporating lithium, sodium, and potassium have emerged as promising candidates for next-generation energy storage due to their high theoretical capacity, energy density, and potential for stable, long-term performance. These batteries operate on mechanisms similar to Li-ion technology but benefit from the greater abundance and lower cost of alkali metals.⁴ The multielectron redox reaction of Se, similar to sulfur, offers a higher theoretical capacity than traditional electrodes, with the potential to overcome the limitations of existing battery systems. Additionally, the abundance of Se in the Earth's crust presents a

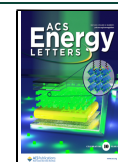
sustainable and eco-friendly alternative to the rare and costly elements used in conventional cathodes.⁵ While selenium is more abundant than lithium, its extraction and processing present environmental challenges. Sustainable sourcing and recycling strategies are crucial to minimizing the ecological footprint, particularly as Se-based batteries scale up for large energy storage applications.⁶ Selenium offers distinct advantages in alkali metal batteries over sulfur as a cathode material, including higher electrical conductivity, which improves electron transport and enables better rate capability. Moreover, selenium-based batteries demonstrate high volumetric energy density, making them ideal for applications where compact, high-energy storage is essential, such as in portable electronics and grid storage. Fully harnessing the potential of Se electrodes requires a deep understanding of the redox mechanisms in alkali metal batteries and the interfacial processes that occur. Understanding the transformations between different Se species during charge and discharge cycles is essential for optimizing battery performance, capacity retention, and overall

Received: March 9, 2025

Revised: April 8, 2025

Accepted: April 9, 2025

Published: April 29, 2025



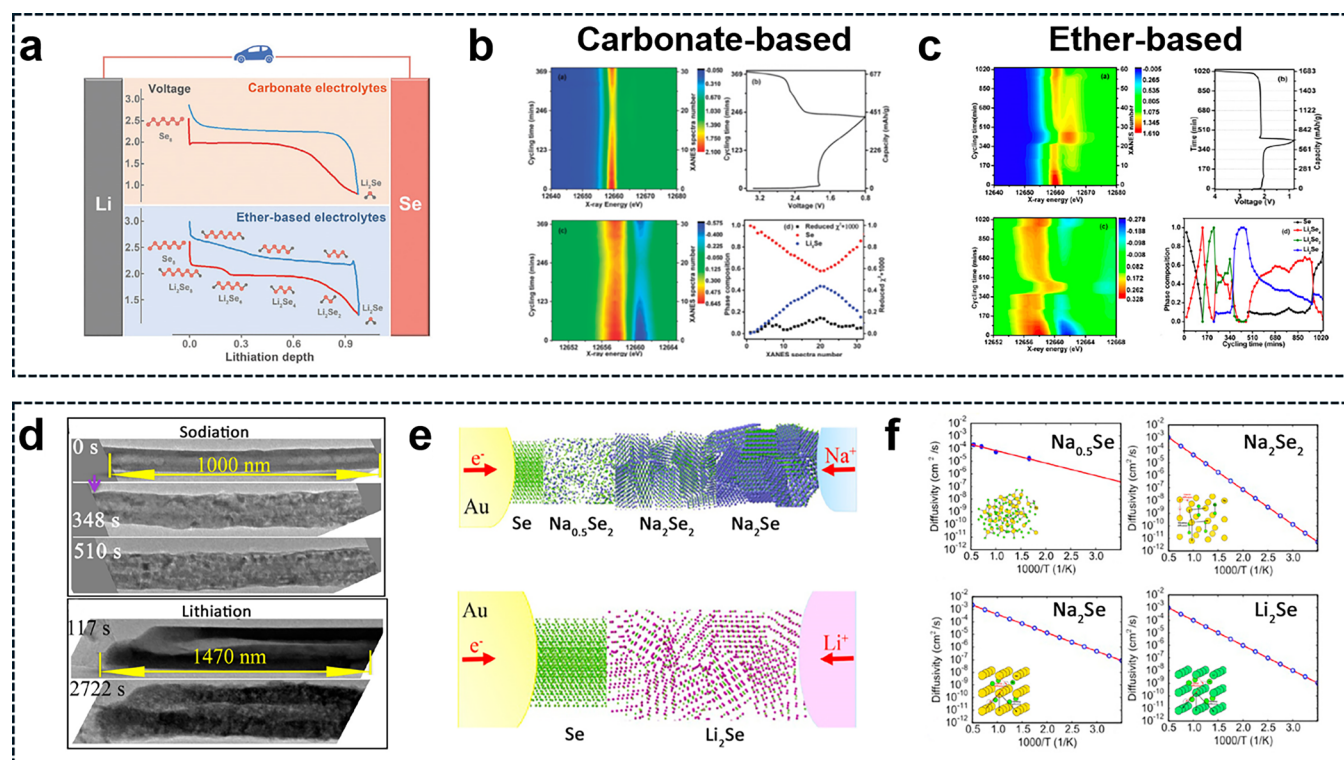


Figure 1. Mechanism of Se in alkali metal batteries. (a) Schematic of Li/Se cell configurations with in-inset voltage profiles using carbonate- (top) and ether- (bottom) based electrolytes.¹² (Reproduced with permission from ref 12. Copyright 2021, John Wiley and Sons) (b) *In situ* XANES measurement for a Li–Se cell using carbonate-based electrolytes, showing normalized XANES spectra (top left), voltage profile (top right), derivative of normalized XANES spectra (bottom left), and linear combination fitting of residue values corresponding to phase composition at different states of charge/discharge (bottom right).¹⁴ (Reproduced with permission from ref 14. Copyright 1996, Royal Society of Chemistry) (c) Normalized XANES spectra of a Li–Se cell in the ether-based electrolyte (top left), voltage profile (top right), derivative of normalized XANES spectra (bottom left), and relative composition evolution of possible phases during cycling.² (Reproduced with permission from ref 2. Copyright 2013, American Chemical Society) (d) Reaction kinetics of Se nanotubes during both sodiation and lithiation processes.⁵¹ (e) Schematic illustration of sodiation and lithiation in Se nanotubes,⁵¹ showing the appearance of three different phases during sodiation and one phase during lithiation. (f) Arrhenius plot of the overall diffusion coefficient of Na-ions in Na–Se phases and Li-ions in Li_2Se phases through a vacancy mechanism.⁵¹ (Reproduced with permission from ref 51. Copyright 2016, American Chemical Society.)

stability. Despite these advantages, selenium-based alkali metal batteries face several challenges that limit their commercial viability. Similar to sulfur-based systems,^{7–11} selenium cathodes experience polyselenide formation and dissolution during cycling, leading to the shuttle effect. This phenomenon causes active material loss, low Coulombic efficiency, and rapid capacity fading. Additionally, reactive alkali metals, particularly lithium, are prone to dendrite formation on the anode, which can result in short circuits and pose safety risks. The dendritic growth of alkali metals under prolonged cycling remains a significant obstacle, impacting both anode stability and overall battery performance. In comparison to conventional lithium-ion batteries, selenium-based systems require innovative solutions in terms of electrolyte design, cathode architecture, and interfacial stability to address these issues. Recent research has focused on strategies such as electrolyte modifications to reduce polyselenide dissolution, advanced cathode architectures to confine active material, and protective layers to stabilize the anode. Overcoming these challenges is crucial to fully realizing the potential of selenium-based batteries and establishing them as viable candidates for clean, high-performance energy storage. This review aims to provide a comprehensive outlook on valuable future research directions by offering a deep understanding of the electrochemical

mechanisms of Se electrodes in alkali metal batteries, thereby promoting their further development.

REDOX MECHANISM

The electrochemical mechanism of Se in alkali metal batteries involves a conversion reaction, where Se is converted to semiliquid polyselenides (PSe_s) and solid metal selenides, similar to the mechanism observed in sulfur electrodes. The redox mechanism of Se depends on the type of electrolyte and the alkali metal used.

Lithium. In Li metal anode–Se cathode systems (LiSeBs) with carbonate-based electrolytes, a solid–solid phase reaction occurs. Conversely, using ether-based electrolytes results in a solid–liquid–solid phase reaction, Figure 1a.^{12,13} Specifically, in carbonate-based solvents, high-order species PSe_s (Li_2Se_n , $4 \leq n \leq 8$) are insoluble, leading to the direct reduction of Se to insoluble low-order species (i.e., $\text{Li}_2\text{Se}_2/\text{Li}_2\text{Se}$), as revealed by X-ray absorption near edge structure (XANES) spectroscopy.¹⁴ Figure 1b shows a counterplot of the Se XANES (top left) and the voltage profile of a Se/Li cell using a carbonate-based electrolyte (top right). The derivative of the XANES spectra (bottom left) and the related Se and Li_2Se phase compositions reveal that the Se edge positions do not shift even at full discharge of the cell (0.8 V), in contrast with Li/Se

system in the ether-based electrolyte, Figure 1c.² Further studies on the Li–Se reaction mechanism in carbonate-based electrolytes revealed different pathways, highlighting the solubility of Se and PSeS.¹⁵ To utilize Se in carbonate-based electrolytes, it was confined within porous carbon nanospheres. The nucleophilic Se anion exhibits high reactivity with carbonyl groups, whereas the shells of the nanospheres protect the reaction of Li_2Se_x with the carbonyl group by forming a passivated film on the surface during the first discharge.¹⁶ In addition to lithiation behavior, the crystal structures of Se formed through various steps were investigated. Typically, Se exhibits three types of crystal structures: trigonal (Se_n , helical polymeric chains), rhombohedral (Se_6 molecules), and monoclinic phases (Se_8 rings with α , β , γ configurations).^{17–20} The Se_8 molecular configuration in chains possesses higher thermodynamic stability than the cyclic Se_8 configuration.²¹ However, amorphous Se (a-Se) exhibits better electrochemical performance than crystalline Se (c-Se).²² The electrochemical performance of a-Se, c-Se, and amorphous/crystalline Se (a/c-Se) cathodes toward Li reveals distinct behaviors.²³ The a-Se and a/c-Se cathodes exhibit a lithiation process at a two-plateau voltage (~ 1.6 and 2.04 V, respectively) through a multistep mechanism. By contrast, the c-Se cathode shows a one-step mechanism with a 1.55 V plateau. The lithiation process in the a-Se process involves Se helical chains that are directly reduced to Li_2Se owing to their active state and the weakened covalent bonds in the Se_n helical chains. Amorphous Se, with its disordered dangling bonds, enables better electrochemical performance and high reactivity with carbonate solvents. However, the strong nucleophilic reaction between chain-like Se and carbonyl groups in carbonate-based electrolytes can lead to capacity fading and short cycle life.⁵ Thus, LiSeBs should be built using amorphous Se cathodes to enhance cell performance. Various strategies to suppress reactivity with carbonyl groups in carbonate electrolytes include designing host materials, nitrogen doping, and incorporating interlayers.^{23–25}

In ether-based electrolytes, the charge/discharge behavior of Se follows a multistep reaction, contrasting with the behavior in carbonate-based electrolytes. The electrochemical mechanism typically involves the conversion of Se to high-ordered PSeS (Li_2Se_n , $4 \leq n \leq 8$), followed by their reduction to low-ordered PSeS (Li_2Se_2 to Li_2Se).^{1–3,26–37} These PSeS are soluble in ether-based electrolytes, leading to shuttle reactions and significant active material loss.³⁸

During discharge, the Se cathode is reduced to Li_2Se_n at approximately 2.1 V, then to Li_2Se_2 , and finally to Li_2Se at ~ 1.9 V. Conversely, during charge, Li_2Se is oxidized to Li_2Se_n ($4 \leq n \leq 8$) at ~ 2.3 V, then to Li_2Se_2 , and eventually back to Se. X-ray photoelectron spectroscopy (XPS) has been employed to investigate the formation of PSeS through electrochemical reactions, revealing that the ring Se_8 oxidizes to chain-like Se_8 after the first charge. In addition, it was investigated the solubility of PSeS in ether-based electrolytes using electrochemical impedance spectroscopy (EIS),³⁹ finding that these electrolytes exhibit higher resistance than carbonate-based ones. This increased resistance is due to the dissolution of PSeS in ether-based electrolytes, which leads to the accumulation of PSeS and increased viscosity. To mitigate the negative impact of polyselenide dissolution on electrochemical performance, various strategies have been explored, similar to those developed for carbonate-based electrolytes.^{13,17,18,24,25,40–42} In line with the general ether electrolyte mechanism, Wu et

al. reported in 2016 the use of Li_2Se nanoparticles as a cathode in a conventional ether-based organic electrolyte. The electrochemical behavior of Li_2Se , akin to that of Li_2S , displays overpotential during the first charge and shuttling of Li polyselenides. This overpotential can be attributed to the difficulty of extracting Li-ions from crystalline Li_2Se and the formation of new interfaces. For pure Li_2Se , a high overpotential of ~ 3.0 V is required, but $\text{Li}_2\text{Se}@C$ composite has a lower overpotential of ~ 2.4 V at an early stage during the first charge. Several clear differences were distinguished between Li_2S and Li_2Se : 1) a lower activation energy barrier for the first charge in Li_2Se compared to Li_2S , and 2) a lower overpotential in the first charge for Li_2Se than for Li_2S . These results stem from the higher electrical conductivity and ionic mobility of Li in Li_2Se than those in Li_2S .⁴³

Similar to Li–S batteries, ether-based electrolytes in Li–Se batteries face significant challenges in suppressing the dissolution of polyselenides. The performance of Se batteries depends significantly on the electrolyte used. Recently, DFT calculations have been employed to analyze the lithiation mechanism in amorphous selenium chains, in particular to explain the two discharge plateaus observed in halide-based systems.⁴⁴ Enhancing battery performance requires a deep understanding of the Se battery mechanism in relation to the electrolyte. Indeed, the process of selenium batteries is similar to that of sulfur both in liquid and solid state. Liquid electrolytes facilitate high ionic conductivity and enable efficient ion transport, but they also promote polysulfide and polyselenide dissolution, leading to the well-known shuttle effect. This shuttle effect occurs as soluble polysulfides migrate between the cathode and anode, causing active material loss, reduced Coulombic efficiency, and capacity fading.^{12,45} Moreover, liquid electrolytes tend to permit dendrite growth on the lithium anode, increasing safety risks and further limiting cycle life. Conversely, in solid-state both batteries, the use of solid electrolytes largely mitigates polysulfide dissolution and the associated shuttle effect.⁴⁶ Solid electrolytes, including sulfides, oxides, and polymer-based types, provide a physical barrier that prevents the migration of soluble polysulfides, thus stabilizing the active material at the cathode. Solid-state configurations also inhibit dendrite growth due to the rigidity of the solid electrolyte, which enhances safety and extends cycle life. However, solid-state electrolytes face challenges related to interfacial resistance, which can impede ion transport and lead to higher overall cell resistance compared to liquid-state systems. Interfacial contact between alkali metal electrode and solid-state electrolyte can be optimized by different approaches including: application of surface coatings (e.g., Li_3PO_4 , Li_3N , etc.) to enhance ion transfer;^{47,48} incorporation of buffer layers (e.g., amorphous oxide or polymer layers) to mitigate mechanical mismatch;⁴⁹ use of soft solid electrolytes or composite layers to improve physical contact and reduce resistance.^{49,50}

Sodium and Potassium. Few studies have reported on the electrochemical mechanisms of Na/K–Se batteries. For example, the mechanisms in carbonate/ether-based electrolytes have not been thoroughly investigated, and partial mechanistic insights remain scarce (Figure 1d–f).^{51–69} As with lithium ions, selenium has alloying reactions with sodium. It undergoes a transformation during sodiation, first forming amorphous $\text{Na}_{0.5}\text{Se}$, followed by polycrystalline Na_2Se_2 and Na_2Se . The initial solid-state amorphization, resulting in $\text{Na}_{0.5}\text{Se}$, is accompanied by a 58% volume expansion. Later, the

recrystallization process leading to Na_2Se_2 and Na_2Se induces a significantly larger volume expansion of approximately 336%.^{51,70}

The reaction kinetics of Se nanotubes with Na and Li have been studied using real-time transmission electron microscopy (TEM) imaging.⁵¹ Sodiation of Se nanotubes occurs 4–5 times faster than lithiation, with the solid-state amorphization process being 10 times more rapid than lithiation. This is attributed to the high electronic conductivity and ionic diffusivity of the Na–Se alloy phases formed during sodiation. This electrochemical behavior is consistent with the observed characteristics of K–Se batteries.^{63,64,66,69,71,72} However, the complete reduction of Se cathodes with K is a complicated multielectron reaction depending on the molecular states of Se.⁶⁶

Studies by Yu et al. reported that no intermediate species formed during the first cycle of K–Se batteries. However, they noted the formation of K_2Se_2 in subsequent cycles, attributing it to incomplete reactions between Se and K, although they lacked direct evidence to support this behavior.⁷³ By contrast, it was proposed that Se directly converts to K_2Se without forming soluble K–PSe.⁷⁴ Sun and co-workers demonstrate for first K–Se batteries using concentrated ether-based electrolytes can follow distinct reaction pathways, involving the reversible conversion reaction from Se to K_2Se_x ($x=5,3,2,1$). The highest voltage plateau of K–Se reaction during charge was found at 1.77 V, slightly higher than that observed with conventional carbonate-based electrolytes (~ 1.5 V). Furthermore, the average voltage plateau during discharge was found at 1.85 V, a value approaching the theoretical predicted by DFT calculations and about 0.5 V higher than previous reported.⁷⁵

Despite these findings, the underlying mechanisms in both ether- and carbonate-based electrolytes for Na/K–Se batteries remain not fully understood. The differences in ionic radii, binding energies, and polyselenide diffusion among Li^+ , Na^+ , and K^+ ions significantly affect the behavior of selenium-based batteries. The larger ionic radii of Na^+ and K^+ result in greater solubility and mobility of polyselenides, leading to an intensified shuttle effect in Na–Se and K–Se systems.

Selenium offers distinct advantages in alkali metal batteries over sulfur as a cathode material, including higher electrical conductivity, which improves electron transport and enables better rate capability.

This increased solubility can improve rate capability by facilitating faster ion transport, but it also presents challenges in retaining active selenium within the cathode, thus impacting long-term cycling stability. Furthermore, energy barriers associated with the reduction of selenium and formation of metal selenides differ across these systems.³ Na–Se and K–Se systems generally exhibit lower energy barriers than Li–Se systems, promoting faster reaction kinetics and higher discharge efficiency.⁴ However, the enhanced diffusion coefficients of Na and K polyselenides, while beneficial for charge transport, also heighten the risk of polyselenide dissolution and migration from the cathode, which can lead to capacity degradation.¹⁸ This comparative analysis under-

scores why Na–Se and K–Se systems may demonstrate superior redox kinetics and energy density compared to Li–Se, yet they require advanced strategies—such as the use of confinement materials, optimized electrolyte formulations, or interlayers—to control polyselenide dissolution and extend cycle life.^{20,45}

Beyond Alkali-Metals. Beyond alkali metal systems, recent studies have explored Mg, Cu, Al, Zn and Ca–Se batteries as promising candidates.⁷⁶ Mg–Se batteries exhibit multiphase discharge behavior, with a faster transformation of high-order PSe to low-order PSe compared to Mg–S batteries.^{77,78} Cu–Se batteries have reported aqueous Se cathode chemistry, where Cu^{2+} acts as the charge carrier, executing a four-electron reaction sequence ($\text{Se} \rightarrow \text{CuSe} \rightarrow \text{Cu}_3\text{Se}_2 \rightarrow \text{Cu}_{2-x}\text{Se} \rightarrow \text{Cu}_2\text{Se}$) during discharge, delivering a high capacity of $\sim 1,350$ mAh g^{-1} .⁷⁹ Shu et al. explored the redox reaction in Cu–Se batteries from investigating the energy level splitting and binding energies using DFT calculations.⁸⁰ Their findings suggest Cu_2Se as the most thermodynamically stable phase in the final discharge product, see Figure S1 a,b in Supporting Information (SI) section. Furthermore, the electrochemical behavior of Al–Se batteries, including Se-based six-electron reaction process ($\text{Se}(-\text{II}) \leftrightarrow \text{Se}(0) \leftrightarrow \text{Se}(\text{IV})$), reveals a superhigh theoretical specific capacity of up to 2,036 mAh g^{-1} .^{81–85} However, these studies have some limitations that need to be addressed in future studies. Amine et al. introduced Al–Se electrochemistry based on two-electron transfer process during reduction of Se to Se^{2-} , demonstrating performance close to the theoretical capacity of Se. The dissociation and association energies of relevant reactants were investigated using first-principles calculations, with a corresponding energy plots reported in Figure S1c in SI section. DFT calculations indicate that compared to TiO_2 (101), Se (101) exhibits a higher adsorption energy and a lower diffusion barrier for $[\text{AlCl}_4]^-$. $\text{TiO}_2@/\text{Se-rGO}$ demonstrates excellent electrochemical performance in Al–Se batteries.⁸⁶ Zhi et al. compared the electrochemical performance of Zn–Se batteries using Se/CMK-3 cathodes in both organic and aqueous electrolytes.⁸⁷ Meanwhile, Zhang et al. reported on the redox mechanism of Se electrodes in Ca-based systems. DFT studies reveals a multistep conversion process involving CaSe_4 , Ca_2Se , and the final product.⁸⁸ This reaction pathway differs from those observed in other Se-metal systems, see Figure S 1d in SI section.

Although the above mechanisms for various cathode-based Se batteries have been suggested, many obstacles and challenges remain in understanding Se batteries, which complicate their commercialization. Extensive research has been conducted using various analyses (such as in situ TEM, Raman spectroscopy, and XRD) to identify the electrochemical mechanism, but no definitive studies have yet been established. In particular, computational analyses, such as DFT calculations, are lacking. Therefore, a more advanced analysis combined with theoretical calculations is required. We believe that studies on Se batteries should incorporate both predictive and supporting experimental results.

Selenium–Sulfur Hybrid Systems. To combine the advantages of sulfur and Se, selenium sulfide (Se_2S) as a cathode for Li/Na– Se_xS_y batteries was reported by Amine's group in 2012.¹ The electrochemical reaction mechanism of Li– Se_xS_y has been extensively investigated.^{1,2,5,27,32,89–97} Similar to Se batteries, Li– Se_xS_y batteries exhibit general

electrochemical reactions depending on the electrolyte solvent (carbonate/ether-based electrolyte). In the carbonate-based electrolyte, Se_xS_y does not form intermediates, whereas, in ether-based electrolytes, it suffers from shuttle problems owing to the dual soluble intermediate polysulfides and PSeS during discharge (Li_2S_n and Li_2Se_n , $4 \leq n \leq 8$) Zhang et al. demonstrated a well-organized Li– Se_xS_y battery system in an ether solvent using operando spectroscopy. This analysis revealed the formation of PSeS during cycling and validated the existence and transformation of enhanced polysulfides and PSeS (Li_2S_n and Li_2Se_n). The formation of Li_2S_n , including Li_2S_8 , Li_2S_6 , and Li_2S_4 was confirmed using Raman spectroscopy. Moreover, peaks corresponding to chain-like Se_n^{2-} (260 cm^{-1}) and the active anion free radical Se^{2-} ($320\text{--}350 \text{ cm}^{-1}$) were observed.⁹⁸ Huang synthesized a few-layered molybdenum sulfide selenide (MoSSe) hybrid electrode by sulfur anion doping in molybdenum selenide-based reduced graphene oxide (rGO). This material consisted of a mixture of 1T and 2H phases. During the initial cycle in Na-half cell, a phase transformation reaction led to the formation of $2\text{H}\text{--}\text{Na}_x\text{MoSSe}$ and $1\text{T}\text{--}\text{Na}_x\text{MoSSe}$, enabling rapid sodium-ion storage.⁹⁹ Yu et al.⁶⁴ developed K– SeS_2 batteries with long cycle life and high energy density by encapsulating SeS_2 in a nitrogen-doped self-supporting carbon nanofiber membrane ($\text{SeS}_2\text{@NCNFs}$). After 1,000 cycles at 0.5 A g^{-1} , the battery exhibited a high reversible capacity of 417 mAh g^{-1} with 85% retention and nearly 100% Coulombic efficiency.⁶⁴ Cui's group developed SeS_2 embedded in ordered mesoporous carbon (named $\text{SeS}_2\text{/CMK3}$) as cathode material, incorporating a foamed copper layer between the cathode and separator to assemble a K– SeS_2 battery.¹⁰⁰ Leveraging the synergistic effects of the $\text{SeS}_2\text{/CMK3}$ structure and the Cu interlayer, a novel Mg– SeS_2 system offering a viable strategy for low-cost, high-area capacity, and high-current rechargeable Mg batteries was proposed. A stainless-steel (SS)-supported lattice-mismatched V–S–Se layered compound ($\text{VS}_y\text{Se}_{2-x}\text{SS}$) with high Se vacancy concentrations was synthesized by tailoring the S-to-Se molar ratio for ultrafast zinc-ion storage. DFT calculations confirmed that Se vacancies significantly reduce the adsorption energy of Zn^{2+} ions on $\text{VS}_{0.5}\text{Se}_{2-x}\text{SS}$, facilitating a more reversible adsorption/desorption process for Zn^{2+} ions.¹⁰¹ Sun et al. successfully addressed the challenge of three-phase interface formation between sulfur, solid electrolyte and the host material ($\text{CoMoS}_2\text{@CNT}$), resulting in the development of high-performance all-solid-state sulfur/ SeS_2 batteries. The battery using SeS_2 as the active material displayed a feasible areal capacity of approximately 3.7 mAh cm^{-2} at 2.0 mA cm^{-2} , retaining 91.8% of its capacity over 400 cycles, highlighting the stable chemistry of the all-solid-state battery featuring $\text{CoMoS}_2\text{@CNT}$.¹⁰² To suppress shuttle reactions, various Se_xS_y -based cathodes employing separator coatings and hosts with carbon and lithiophilic characteristics have been reported.^{89,98,103–106} Studies using solid electrolytes to prevent the dissolution of PSeS in liquid electrolytes have also been reported. PSeS are absent during cycling in all-solid-state batteries (ASSBs) that employ solid electrolytes. This suggested a one-step reaction between $2\text{Li} + \text{Se} \rightarrow$ and Li_2Se . Li et al. first reported an ASSB using $\text{Se}\text{--}\text{Li}_3\text{PS}_4\text{--}\text{C}$ as the cathode, Li_3PS_4 as the electrolyte, and a Li–Sn alloy anode.¹⁰⁷ They demonstrated the conversion of Se into Li_2Se during discharging and the recovery of Se after charging using ex situ X-ray diffraction (XRD) and Raman analyses.

COMPUTATIONAL AND EXPERIMENTAL SE-ELECTRODE DESIGN

Structural Design and Cathode Composition. As discussed in the previous chapter, studies on Se electrodes in alkali metal batteries showed mechanisms and chemistry similar to those of S electrodes, while exhibiting different chemical and physical properties.^{31,108} First, compared to sulfur, Se has a much higher electrical conductivity (10^{-4} vs $10^{-15} \text{ ohm}^{-1} \text{ cm}^{-1}$), which promotes kinetics and electrochemical reactions with alkali metals, reduces the need for conductive additives, and allows for greater active material loading in the cathode. Second, the redox mechanism involving the formation of polysulfide/selenides and the associated “shuttle effect” to the negative electrode surface is less pronounced in Se, resulting in fewer parasitic reactions and reduced active material loss. Finally, the electrochemical potential toward alkali metals is 0.5 V higher for Se than for S, which increases the energy density in electrochemical redox devices.¹⁰⁹ Despite the “shuttle effect” being less pronounced in Se-based batteries, it remains a notable challenge. For example, the use of pure nanoporous Se as a cathode in Li-ion systems has demonstrated low cell performance owing to pronounced shuttle-side reactions.¹¹⁰ Different approaches have been adopted to mitigate the “shuttle effect”³ and one of the most exploited is the physical entrapment of Se in porous hosts. Similar to S electrodes,¹¹¹ significant efforts have focused on the synthesis and optimization of conductive porous carbon hosts. The porosity of the host material plays a key role in various functions: (i) enhancing electronic conductivity, (ii) confining an adequate amount of active material at the cathode, (iii) immobilizing high-order selenides to prevent the shuttle effect and loss of the active material, and (iv) accommodating the volume changes of Se during electrochemical reactions with alkali metals. The design of porous carbon structures plays a critical role in optimizing Se electrode performance, but factors such as size, distribution, and morphology are equally important.¹¹² Various studies have investigated Se confinement in micropore ($d < 2 \text{ nm}$)^{16,26,53,54,57,63,113–117} and mesoporous ($2 < d < 50 \text{ nm}$)^{3,75,118–122} matrices. Materials with micropores efficiently confine Se within the cathode, limiting PSeS dissolution. However, they have inherent limitations regarding active material loading. For example, Na–Se batteries utilizing microporous cellulose-derived carbon nanosheets (CCNs) confined with 53% w/w demonstrated a reversible capacity of 613 mAh g^{-1} at 0.1C and 296 mAh g^{-1} at 10C over 500 cycles. In comparison, mesoporous carbon can load a higher content of Se but generally exhibits poorer cycle performance. For example, Se was confined to mesoporous nanocellulose-derived monolithic carbon ($\text{Se}\text{--}\text{NCCMC}$) cathodes in Na–Se batteries, achieving a Se loading of 70 wt %; however, the reversible capacity for Na storage was 511 mAh g^{-1} with 98% retention over 150 cycles.¹²³ Hierarchical microand mesoporous carbon hosts have been proposed to confine more active materials to the electrodes.^{15,25,56,65,69,71,124–130} This high-Se electrode was further enhanced by heteroatom doping of the carbon matrix (such as N, O, B, and S).

Using density functional theory (DFT), Islam et al. investigated the binding mechanism of Li_2Se_n on graphene and surface-functionalized Ti_3C_2 MXenes. Graphene was used as a reference material to evaluate the binding strengths of Li_2Se_n on functionalized $\text{Ti}_3\text{C}_2\text{X}_2$ (where X = S, O, F, and Cl).

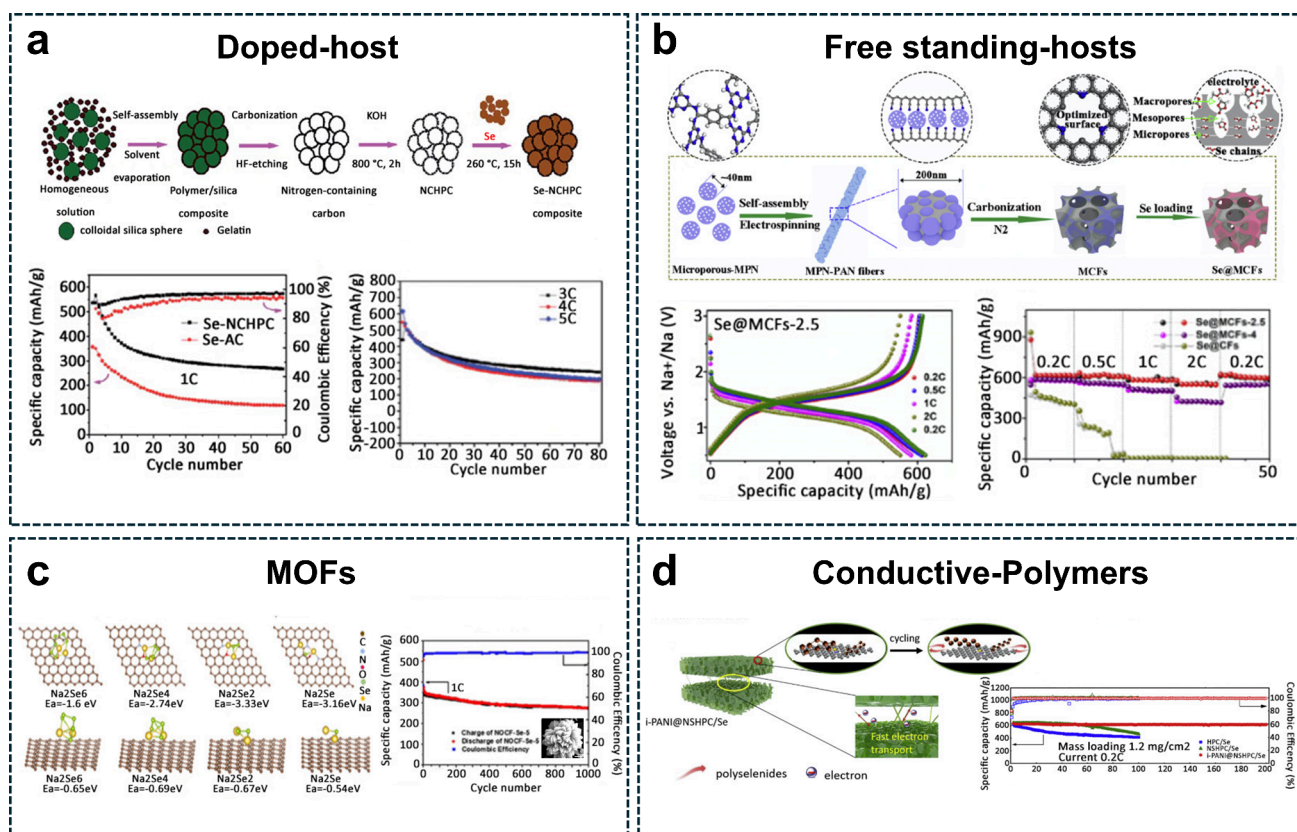


Figure 2. Se electrode design. (a) Schematic illustration of the synthesis procedure (top) for Se-NCHPC, TEM images (bottom left), and the corresponding elemental mapping of C (red), N (orange), and Se (green). Cycling performance (bottom right) of Se-NCHPC and Se-AC in Li/half cells at a current rate of 1C (675 mA g^{-1}).¹³⁷ (Reproduced with permission from ref 137. Copyright 2012, Royal Society of Chemistry) (b) Synthesis of free-standing N-doped Murray carbon framework with high Se-loading (top). SEM and STEM images with related EDX mapping of C (yellow), N (red), O (green), and Se (blue). Voltage profiles of the Se@MCF-2.5 cathode and related rate performance (bottom right) in Na/half cells.¹²⁶ (Reproduced with permission from ref 126. Copyright 2021, Elsevier) (c) Adsorption energy of Na-polysulfide calculated through DFT analysis (left). Cycling performance of Se codoped porous flower electrode in Na-based cells.⁶⁰ (Reproduced with permission from ref 60. Copyright 2022, Elsevier) (d) Electrochemical performance of Se-composite with aniline-based polymer in Na-half cells at a current density of 0.2C.¹⁴⁸ (Reproduced with permission from ref 148. Copyright 2019, Elsevier.)

The calculated adsorption strengths of Li_2Se_n on S^- and O^- terminated Ti_3C_2 were found to be higher than those of commonly used ether-based electrolytes, a crucial factor in effectively suppressing Li_2Se_n shuttling.¹³¹ Furthermore, electronic density distribution studies on the 3DG-CNT@Se material revealed a significant electron density in the interaction between selenium and graphene, suggesting strong chemical bonding.¹³² Wu et al. developed a lignin-derived dual-doped (O and S) hierarchical porous carbon as a selenium host and confirmed, via DFT calculations, the strong affinity of selenides for O and S sites, which help in mitigating the shuttle effect.¹³³ As a result, the Se electrode exhibited exceptional cycling stability, retaining a high capacity of 460 mAh g^{-1} after 500 cycles at 0.5 C. Similarly, Li's group synthesized sulfur- and oxygen-co-doped hierarchical porous carbon (SO-HPC) through carbonization and activation. DFT calculations revealed that the binding energy of Li_2Se to S,O-co-doped carbon was significantly higher than that of either S-doped or O-doped carbon alone, indicating enhanced chemisorption of polyselenides and Li_2Se . Consequently, the assembled Li-Se batteries demonstrated remarkable performance under extreme temperatures, maintaining capacities of 394 and 264 mAh g^{-1} after 400 cycles at 0.5 C at 50 and 0 °C, respectively.¹³⁴

Recently, using DFT calculations it was demonstrated that 2D $\text{Ti}_3\text{C}_2\text{T}_x$ MXene, with its polar interfaces effectively facilitates the chemical immobilization and physical blocking of polyselenides, thereby suppressing the shuttle effect. The unique architecture of $\text{Ti}_3\text{C}_2\text{T}_x$ MXene, integrated atop interlinked nanofibers, ensures continuous electron transfer for redox reactions. As a result, the novel Janus PNCNFs/Se@MXene electrodes exhibit exceptional rate capabilities and long-term cycling stability in both Na-Se and Li-Se batteries.¹³⁵ Additionally, to gain deeper insights into the superior electrochemical performance of Se@NOPC-CNT films as cathodes for Na-Se and K-Se batteries, further studies were conducted.⁷³ Furthermore, DFT calculations were performed to model the adsorption behavior of $\text{Na}_x\text{Se}/\text{K}_x\text{Se}$ ($0 < x \leq 2$) on three different substrates: pristine carbon (C), O-doped carbon (OC), and N,O dual-doped carbon (NOC). First-principles calculations at various sodiation stages revealed that the binding energies between $\text{Na}_2\text{Se}/\text{Na}_2\text{Se}_2$ and C, OC, and NOC are $-0.41/-0.43$, $-2.16/-2.90$, and $-4.08/-4.94$ eV, respectively, indicating that OC has a stronger binding affinity than pure C but lower than NOC. A similar trend was observed for $\text{K}_2\text{Se}/\text{K}_2\text{Se}_2$. These findings confirm that N,O dual-doping significantly enhances the chemical affinity between $\text{Na}_2\text{Se}/\text{Na}_2\text{Se}_2$ (and $\text{K}_2\text{Se}/\text{K}_2\text{Se}_2$) and the modified carbon matrix, thereby improving electrochemical perform-

ance.⁷³ Hu et al. designed a cobalt selenide-sulfide (CoSe₂–CoS₂) Mott–Schottky heterostructure catalyst on carbon fibers (CoSe₂–CoS₂@CNF). By leveraging the built-in electric field and high catalytic activity of the heterostructure, the CoSe₂–CoS₂@CNF effectively reduces the nucleation barrier for polyselenides, enhances the liquid–solid conversion process, and facilitates ordered radial deposition of polyselenides on the carbon fibers. DFT calculations, supported by Gibbs free energy analysis, further demonstrate that the CoSe₂–CoS₂ Mott–Schottky heterostructure exhibits the highest catalytic activity, accelerating the rapid conversion of polyselenides.¹³⁶

Polar Modification of Cathodes. The presence of heteroatoms improves the binding of polar polyselenide species during the electrochemical process and limits shuttle-side reactions, thus enhancing the battery performance.¹³⁷ Qu et al. reported a novel nitrogen-containing hierarchical porous carbon (NCHPC) to confine Se in Li–Se batteries. Figure 2a shows the synthesis process, which involves the carbonization of a polymer/silica composite, followed by HF etching and mixing with elemental Se.¹³⁷ In the final composite, Se was homogeneously distributed within the carbon host, as confirmed by TEM images and corresponding elemental mapping. From an electrochemical perspective, the authors revealed that the Se–NCHPC composite cathode exhibited a higher reversible capacity (267 mAh g^{−1} after 60 cycles at 1C) compared to a conventional Se/C material. Additionally, the cathode maintained a consistent capacity of approximately 240 mAh g^{−1} across varying current rates, including 3C, 4C, and 5C, showcasing its robust performance under high-rate conditions.

N-containing hollow-core mesoporous-shell carbon spheres (NHCS) demonstrated high anchoring of Se at the cathode side in Li- and Na-based batteries.¹³⁸ A 72 wt % Se-active material was loaded into the NHCS while maintaining excellent cyclability. Freestanding materials have also been proposed by designing hierarchical micro/meso/macroporous compounds composed of N-doped carbon fibers (MCFs). Dong et al. reported the benefits of free-standing electrodes, showing a potential path to reduce inactive material in the Se electrode, reaching a loading of 60 wt % of active material with good capacity retention even at 5C-rate, Figure 2b, ensuring optimal electron and ion transport, as well as Se structural stability.¹²⁶ The synthesis procedure involved the electrospinning of microporous nanoparticles, followed by carbonization, and subsequent Se infiltration in an autoclave. Scanning electron microscopy (SEM) images show the nanofiber morphology, while energy dispersive X-ray spectroscopy (EDX) maps confirm a uniform distribution of all elements. Electrochemically, the Se@MCF-2.5 cathode shows stable voltage profiles as the current density increases from 0.2 to 2C, achieving discharge capacities of 606, 605, 580, and 550 mAhg^{−1} at 0.2, 0.5, 1, and 2C, respectively.

In addition, significant attention has been given to the application of metal–organic frameworks (MOFs) that contain metals. These MOFs are noted for their high surface areas and regular, uniform atom distributions, contributing to their potential as advanced porous structures for battery applications. The favorable characteristics of these frameworks include the ability to tune their composition by selecting appropriate metals and organic ligands.¹³⁹ MOFs can also be doped with abundant heteroatoms, which can enhance their electronic conductivity. Additionally, MOFs possess good hydrophilicity

and confinement capabilities,¹⁴⁰ ensuring fast diffusion of ions and electrons.^{52,74,90,141–146} An N/O codoped flower-like porous host was developed from a Ni-MOF precursor, followed by Se infiltration using two different methodologies: melt diffusion and vapor infiltration.⁶⁰ The vapor infiltration method yielded the best electrode homogeneity by avoiding Se aggregation and achieving an overall loading of 63 wt %. In addition, density functional theory calculations highlighted that the increased polarity of the carbon matrix due to O doping enhances the adsorption of Se and PSe_s. The performance of the Se electrodes in Li-ion cells showed a capacity of 334 mAh g^{−1} at 0.1C and maintained good reversibility at a 1C rate for over 1,000 cycles, Figure 2c. Transition metal oxides with highly polar surfaces and tunable architectures hold great potential for suppressing intermediate shuttling in Li–Se batteries. To provide guidance for developing metal compound hosts for Li–Se batteries (LSeBs), Choi et al. conducted a computational screening of transition-metal disulfides using DFT calculations. Their study revealed that group IV and V disulfides—specifically VS₂, NbS₂, TaS₂, TiS₂, ZrS₂, and HfS₂—exhibit superior polyselenide entrapment compared to group VI disulfides such as CrS₂, MoS₂, and WS₂. Among them, NbS₂, TaS₂, and TiS₂ emerged as the most promising candidates due to their significantly stronger affinities for polyselenides.¹⁴⁷ Conductive polymers can also serve as additives to address the PSe_s shuttle effect and dissolution issues, thereby increasing overall electronic conductivity.^{148–152} In particular, polymers with heteroatoms (e.g., O, S, N) and a highly extended π -delocalized system have been employed to improve Se-electrodes. Zhang et al. reported the designed architecture of an N, S-dual-doped hierarchical porous carbon/Se composite coated with interconnected polyaniline, Figure S2 in SI section and Figure 2d.¹⁴⁸ The carbon host was synthesized by the carbonization of sodium citrate and thiourea, followed by KOH activation. The N, S-doped C/Se composite was obtained via a simple melt diffusion method. Finally, a polyaniline (PANI) layer with an interconnected structure was grown via the *in situ* polymerization of aniline, resulting in a uniform elemental distribution of C, N, S, and Se, as shown in Figure 2d, which shows the high-resolution transmission electron microscopy-energy dispersive X-ray spectroscopy (HRTEM-EDS) technique. The cycling performance of the composite showed an outstanding capacity retention of 97.3% after 200 cycles, compared to carbon hosts without conductive polymers. The interconnected PANI layer effectively traps PSe_s within the carbon matrix and acts as a diffusion barrier. Furthermore, the interconnected structure enhances conductivity by linking individual particles, resulting in excellent electrochemical performance. Recent advancements include synthesizing PANI interconnected with the porous carbon matrix of the host through *in situ* polymerization¹⁴⁸ or polyacrylonitrile (PAN) fibers through the pyrolysis of PAN/SeS precursors.¹⁵³ Transition metals such (M_xO_y/Se),^{150,154–157} metal selenides (MSe),^{78,84,85} and MXenes (M_{n+1}C_nT_m)^{131,135} have also been investigated for cathodic materials. Introducing metal oxides such as TiO₂, Al₂O₃, NiO, SnO₂, and ZnO improves the polarity of the Se host and facilitates electrostatic interactions with PSe_s.¹² Although oxides offer good adsorption properties for PSe_s, their low electronic conductivity can limit the rate capability of Se electrodes, necessitating additional conductive additives. A 3D Ni foam foil interlayer was used to improve the electronic properties of the Se/TiO₂ porous fiber composites,

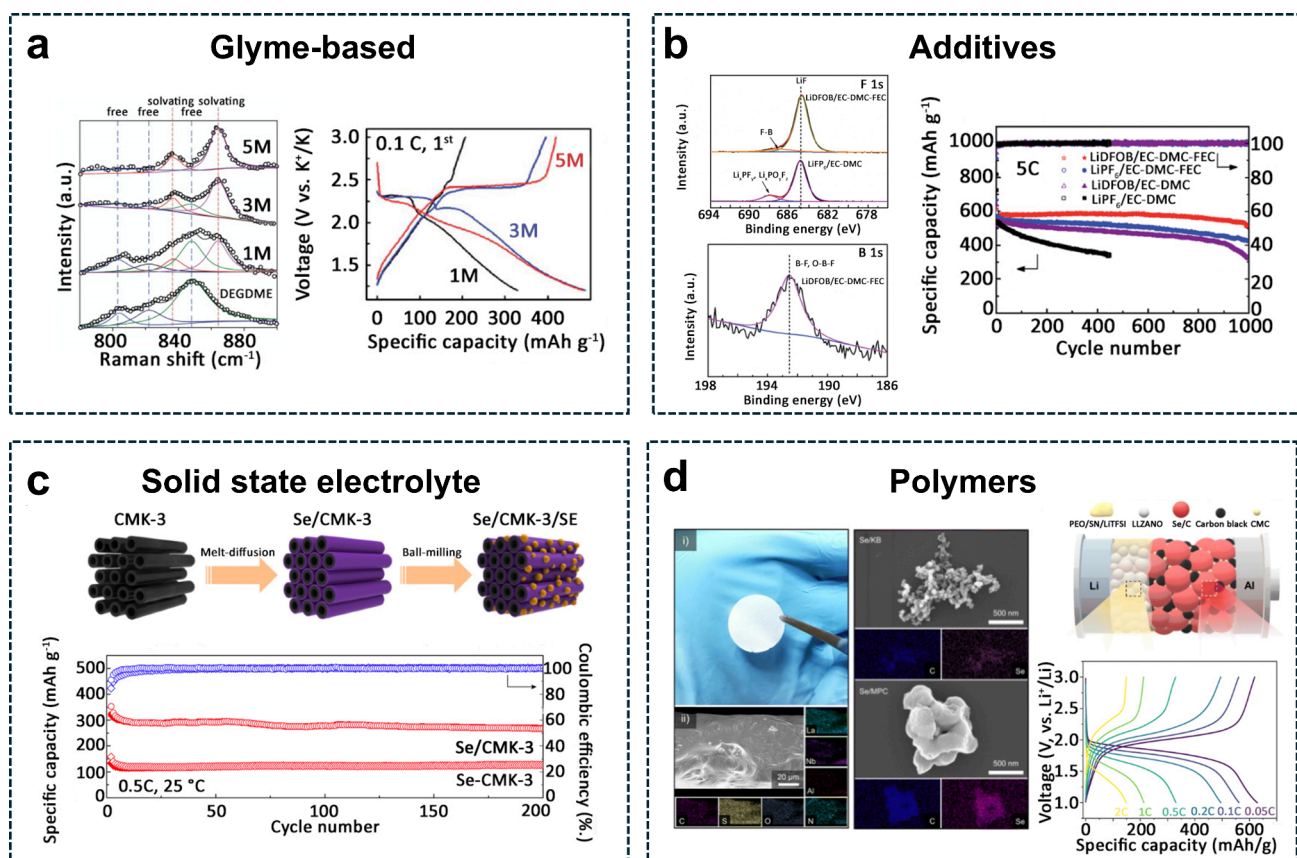


Figure 3. Electrolyte design. (a) Liquid electrolyte: (left) solvation discrepancies revealed by Raman spectra analysis of DEGDMC ether-based electrolytes with KTFESI salt concentrations of 1, 3, and 5 M. (Bottom left) Voltage profiles of K–Se cells using KTFESI salt at different concentrations.⁷⁵ (Reproduced with permission from ref 75. Copyright 2010, Royal Society of Chemistry) (b) Additives: Galvanostatic performance of Li–Se cells with different electrolyte configurations including additives at a 5C-rate (1C = 678 mA g⁻¹); X-ray photoelectron spectra at the F 1s core level. X-ray photoelectron spectra at the B 1s core level for the cycled Se/MC cathode using LIDFOB/EC-DMC-FEC and LiPF₆/EC-DMC electrolytes.¹¹⁵ (Reproduced with permission from ref 115. Copyright 2012, Royal Society of Chemistry) (c) Solid-state electrolyte: (Top) Synthesis of Se/CMK-3 and mixing with solid-state electrolyte. (Bottom) Cycling performance of Li-battery using Li₁₀GeP₂S₁₂ solid-state electrolyte with mixed Se-CMK-3 and annealed Se/CMK-3 at a 0.5C rate and 25 °C.¹⁶⁸ (Reproduced with permission from ref 168. Copyright 2020, American Chemical Society) (d) Composite polymer: (Top left) visual image of a poly(ethylene oxide) (PEO/LLZANO/LiTFSI/SN-CPE) disk. CPE surface morphology and elemental mapping by EDS. Micromorphologies and EDS elemental mapping results of Se/KB and Se/MPC cathode materials. (Top right) Scheme of cell configuration and (bottom right) rate capability test of the cell using modified polymer electrolyte.¹⁷⁹ (Reproduced with permission from ref 179. Copyright 2024, Royal Society of Chemistry.)

thereby enhancing both electrode cyclability and electronic conductivity.¹⁵⁶ Another strategy involves the use of a facile deposition technique, namely, atomic layer deposition (ALD), which creates highly uniform thin oxide layers on conductive surfaces. Microporous carbon–Se electrodes were protected using a Al₂O₃ thin layer in a Na–Se battery configuration.¹⁵⁷ The thickness of the metal oxide layer significantly influenced the battery performance, with the optimal result achieved using 10 ALD cycles, promoting the formation of a stable solid electrolyte interface (SEI) layer with fast diffusion of electrons and metal ions. The reversible discharge capacity achieved was 664 mAh g⁻¹ at the second cycle, with an 86% retention over 100 cycles. MSeS show similar issues related to low conductivity, necessitating the use of additional conductive agents (e.g., porous carbon hosts, carbon nanostructures, and fibers). Despite these challenges, MSe compounds offer significant advantages, such as high specific capacity, low cost, tunability, and catalytic properties, with performance varying based on the type of transition metal used.^{158,159} A notable development in this area is the N-doped porous carbon/ZnSe nanoparticle composite, specifically designed for

Zn–Se batteries.⁸⁴ The composite achieved an initial discharge capacity of 172.6 mAh g⁻¹ at a current of 300 mA g⁻¹ and maintained a capacity of 70.4 mAh g⁻¹ after 250 cycles at 500 mA g⁻¹ with a discharge voltage of 1.8 V. Although far from the performance in Li or Na-based systems, these results are remarkable compared to other similar works based on Al-storage. The mechanism based on the conversion-alloying reaction was confirmed by ex situ XRD and X-ray photoelectron spectroscopy (XPS) analyses. The results reported using Al anodes are still far from those of other chemistries and need to be widely investigated in the future, both in terms of cell performance and mechanism. To enhance electrical conductivity, surface area, and catalytic properties for promoting PSeS adsorption in alkali-Se batteries, researchers have explored MXene-based compounds. This approach leverages a broad range of 2D materials, including transition-metal carbides, nitrides, and carbonitrides.¹⁶⁰

A notable example involves incorporating Ti₃C₂T_x MXene into Se-infiltrated porous pyrrolic-N-doped carbon nanofibers to create a freestanding cathode for Na-ion batteries.¹³⁵ This design demonstrated a reduction in electron transfer resistance

(Rct), which improved charge-transfer kinetics. DFT calculations showed that pyrrolic N significantly enhances PS adsorption. The Na-battery delivered a reversible capacity of 348 mAh g⁻¹ at 10C after 5,000 cycles, and the cathode maintained a capacity of 411 mAh g⁻¹ even at 20C.

■ ELECTROLYTIC CONFIGURATIONS FOR ALKALI SE METAL BATTERIES

Material Selection for Electrolyte and Formulation.

The electrolyte is a key component of rechargeable batteries, as it significantly affects both the interface at the electrode surface and the overall safety of the device. In Se-alkali metal batteries, low-cost carbonate-based electrolytes can be used with mesoporous carbon-confined elemental Se as the working electrode. However, this combination often results in poor electrochemical performance and rapid capacity fading. To avoid capacity fading, more complex electrodes, such as Se/MWCNT cathodes, are employed in Li-ion cells with an ethylene carbonate/ethylmethyl carbonate (EC/EMC) 1.2 M LiPF₆ electrolyte mixture.¹⁴ Capacity fading was investigated through in situ X-ray diffraction (XRD) and X-ray absorption spectroscopy (XPS) analyses, highlighting that the Se crystal structure plays a critical role in the electrochemical performance and capacity fading.²³ Similar to S-based systems, the use of ether-based electrolytes is also suggested as they can favor the formation of a uniform and compact solid electrolyte interface (SEI), thus preventing the uncontrolled growth of metal dendrites at the anode side.^{27,161} Potassium bis-(trifluoromethylsulfonyl)imide (KTFSI)-diethylene glycol dimethyl ether (DEGDME) electrolytes with different salt concentrations (i.e., 1, 3, and 5 M) have been proposed. Raman spectra showed that the intensity of the three vibrational bands associated with DEGDME molecules decreased as the salt concentration increased. Conversely, the Raman signals of solvated DEGDME showed an increasing trend, indicating that at higher salt concentrations (≥ 3 M), the solvent molecules were coordinating with K⁺ ions, rendering them less available for the PSes shuttle effect.⁷⁵ Although the viscosity of the electrolyte increased with higher salt concentrations, leading to reduced ionic conductivity, K⁺ ions maintained rapid migration even at 5 M KTFSI, **Figure 3a**. The 5 M electrolyte demonstrated higher specific capacity and better capacity retention compared to the 1 and 3 M electrolytes. Indeed, lower electrolyte concentrations increased the dissolution of redox intermediates, as confirmed by the average Coulombic efficiency (CE) beyond 100% in the 1 and 3 M electrolytes.

Similar results can be achieved by coupling highly salt-concentrated ether-based electrolytes with additives such as fluoroethylene carbonate (FEC)¹⁶² and/or LiNO₃,¹⁰³ which react at the anode surface to form an SEI layer that protects the surface against PSes deposition. Similar approaches have also been used in carbonate-based electrolytes to study Li–Se battery performance with different LiDFOB/FEC combinations in EC/DMC.¹¹⁵ These results highlight the synergistic effect promoted by the LiDFOB/FEC coupling additives on the capacity and electrochemical stability, which were further analyzed through SEM and XPS characterizations, **Figure 3b**.¹¹⁵ When the cathode was tested at a high current (5C) during the rate capability test, the beneficial effects of both additives were clear. The capacity retention was approximately 88% after 1,000 cycles (511 mAh g⁻¹) for LiDFOB/EC/DMC-FEC, corresponding to a capacity decay of only 0.012% per

cycle. Conversely, electrolytes without additives and those with only FEC or LiDFOB showed the worst performance. The authors attributed these variations in the stability of SEI on the surface of the Li anode and cathode. SEM images showed a compact and smooth Li deposition morphology for LiDFOB/EC-DMC-FEC, compared to the rough and spongy morphology observed with LiPF₆/EC-DMC. The introduction of FEC promoted greater compactness, while substituting LiPF₆ with LiDFOB helped prevent the formation of Li dendrites. XPS analysis of the Se/microporous carbon cathode revealed the SEI composition in the LiDFOB/EC-DMC-FEC system, highlighting the presence of LiF, F–B, and O–B–F species. These components are beneficial for protecting both the anode and cathode by suppressing side reactions and enhancing the electrode kinetics **Figure 3b**.

The risks of explosion and flammability are significant considerations when designing organic solvent-based electrolytes, where both the solvent and salt play crucial roles. Chlorate-based salts, known for their explosive nature, are no longer recommended for use in electrochemical devices.¹⁶³ Valid alternatives include solid-state electrolytes, which fall into two major categories: inorganic and organic. Common inorganic solid electrolytes include perovskites, garnets, Na/Li superionic conductors (NASICON and LISICON, respectively), and sulfide-based electrolytes. These materials are known for their excellent cationic conductivity, high thermal stability, and lack of metal dendrite formation.¹⁶⁴ They can also prevent shuttle reactions and PSes formation when coupled with Se systems. A Li–Se battery using a solid sulfide electrolyte has advantages in stabilizing the Se electrode performance.¹⁰⁷ Another promising alternative is related to ionic liquid (IL)-based electrolytes, which are nonflammable, low volatility, and thermally stable electrolytes. Molecular dynamics simulations have investigated Na⁺ transport in various ILs, revealing that cation additives like Li⁺, K⁺, and Ca²⁺ can improve stability **Figure S3a** in SI section.¹⁶⁵ Among these, Li⁺ has been identified as the most effective in reducing electrolyte decomposition and enhancing Na-ion transport, offering a viable strategy for stabilizing Na metal anodes **Figure S3b-d** in SI section.¹⁶⁶

In summary, for carbonate-based electrolytes, cathodes with stabilized, encapsulated selenium structures are particularly suitable. Carbonate electrolytes are known to react with free selenium or soluble polyselenides, leading to unwanted side reactions and capacity fade. To mitigate this, selenium is often encapsulated within conductive matrices, such as carbon frameworks or polymer coatings, which act as physical barriers to reduce direct contact between the electrolyte and active selenium. For example, selenium encapsulated in porous carbon or mesoporous structures has shown good compatibility with carbonate electrolytes, as these matrices limit polyselenide dissolution and improve structural stability during cycling.^{16,18} Additionally, cathodes with protective coatings, such as metal oxides or conductive polymers, provide a secondary layer that can further reduce reactivity and help maintain stable cycling performance in carbonate systems.^{3,45,167} In contrast, ether-based electrolytes are more compatible with cathodes that employ polyselenide confinement strategies. Ether solvents exhibit greater polyselenide solubility, which supports a higher sulfur loading and enhances redox kinetics. In ether-based systems, the use of carbon hosts and confinement structures, such as metal–organic frameworks (MOFs) or conductive polymers, effectively trap dissolved

polyselenides within the cathode, reducing their migration and enhancing cycling stability.

Interface Engineering in Electrolytes. State-of-the-art solid electrolytes face challenges related to high interfacial resistance and cracking of the electrolyte pellets owing to stress and strain during electrochemical reactions.^{168–170} This resistance impedes ion transport across the solid–solid boundary, reducing overall cell conductivity and rate capability. The rigid structure of solid electrolytes can also limit interfacial contact, especially as electrodes undergo volume changes during cycling, which exacerbates resistance and contributes to capacity fade.^{171–173} Mechanical and chemical stability issues also affect performance. For example, sulfide-based electrolytes are prone to chemical reactions with lithium–metal anodes, forming interphases that increase resistance and reduce ionic conductivity. Furthermore, the mechanical stress from volume expansion and contraction during cycling can lead to cracks and delamination at the interface, affecting overall stability. Oxide-based electrolytes are chemically stable but suffer from limited mechanical flexibility, which may lead to gradual interfacial degradation over repeated cycles.¹⁷⁴ Another challenge is SEI formation and ion transport. Unlike liquid electrolytes, where stable SEI layers can form naturally, solid-state systems face difficulties in establishing an ideal SEI layer at the interface. While artificial SEI layers have been explored to stabilize these interfaces, creating a conductive, robust SEI across a solid–solid boundary remains challenging.⁴⁶ Inorganic solid-state electrolytes play a crucial role in addressing the challenges of polyselenide migration and overall stability in selenium-based batteries. They act as physical barriers that confine polyselenides within the cathode, preventing their migration to the anode and effectively mitigating the shuttle effect. For example, sulfide-based solid electrolytes create impermeable layers that limit polyselenide dissolution, ensuring better retention of active materials.^{175,176} Additionally, oxide-based inorganic electrolytes are chemically stable, avoiding reactions with polyselenides and forming passivating layers on the anode to suppress cross-contamination and unwanted side reactions. These electrolytes also facilitate efficient lithium-ion transport while blocking polyselenide migration, providing high ionic conductivity and minimizing active material loss.^{175,176} Furthermore, ceramic electrolytes inhibit dendrite growth on the anode through their rigid structures, stabilizing the anode and indirectly reducing the shuttle effect by limiting the reactive surface area. Collectively, these properties highlight the effectiveness of inorganic electrolytes in improving the performance and stability of selenium-based batteries.^{177,178} Hybrid approaches, such as introducing a thin liquid or polymer layer between the solid electrolyte and electrode, have shown promise in reducing interfacial resistance and facilitating ion transport. One addressed these issues by using ordered mesoporous carbon (CMK-3) combined with Se and a solid electrolyte to mitigate volume expansion and reduce interfacial stress, **Figure 3c**.¹⁶⁸ Se/CMK-3 composites were mixed with Super P conductive material and a LISICON-based electrolyte, specifically $\text{Li}_{10}\text{GeP}_2\text{S}_{12}$, through ball milling to promote interface contacts and enhance electron/ion conductivity.

The Li-ion solid-state cell built with this electrolyte showed a reversible capacity of 488.7 mAh g⁻¹ after 100 cycles at a 0.05C-rate. Even at a higher current rate of 0.5C, the Se/CMK-3 composite achieved a specific capacity of 269 mAh g⁻¹,

Figure 3c, with significantly reduced ohmic resistance because of improvements in both electronic and ionic conductivity.

Organic solid electrolytes are solid conductive polymers that suffer from very low ionic conductivities at room temperature, necessitating higher working temperatures to ensure good ion transportation. Using fillers in the polymeric composition (e.g., inorganic nanoparticles, organic plasticizers, and cross-linkers) can enhance the ionic conductivity, but the ionic conductivity still falls below the benchmark value of 10⁻³ S cm⁻¹ for practical applications.¹⁹³ Gel polymer electrolytes, formed by adding liquid electrolytes to a solid polymer matrix, can be used in Se-based batteries with good ionic conductivity at room temperature.^{180,181}

The coupling of composite polymer electrolytes with Se batteries has been designed to achieve high energy density, low operational temperature, easy manufacturing, and good electrochemical stability, **Figure 3d**.¹⁷⁹ A composite polymer electrolyte (CPE) compatible with a Se–C electrode can be prepared using poly(ethylene oxide), $\text{Li}_{6.25}\text{La}_3\text{Zr}_2\text{Al}_{0.25}\text{Nb}_{0.25}\text{O}_{12}$ (LLZANO) as a ceramic filler, lithium bis(trifluoromethanesulfonyl)imide (LiTFSI) as a Li salt, and succinonitrile (SN) as a plasticizer. The morphology and microstructure of LLZANO were examined using SEM and energy dispersive X-ray spectroscopy (EDS), respectively. LLZANO is composed of 5–8 μm particles with even distributions from La, Zr, Al, and Nb. The reduction in the crystalline area increased the amorphous content, promoted greater segmented polymer motion, and enhanced ionic conductivity. Thus, the addition of LLZANO improves the ionic conductivity of the solid electrolyte, **Figure 3d**. The micromorphology of the Se/C composites was identified using SEM images. The corresponding EDS results confirmed the uniform dispersion of Se within the host material. The rate capability test of the Se/C composite in a Li-half cell with a CPE electrolyte showed good performance, with capacities ranging from 640 to 150 mAh g⁻¹ at rates between 0.05 and 2C respectively (1C = 675 mA g⁻¹) and 25 °C, **Figure 3d**. **Table S1** in SI section, summarizing the advantages and disadvantages of different electrolyte systems has been added to provide a clear and concise overview. The table includes key points for carbonate-based, ether-based, solid-state, and hybrid electrolytes, reporting their benefits and limitations for selenium-based batteries. Among the others, polyselenide dissolution in liquid electrolytes leads to the shuttle effect, causing capacity loss, low efficiency, and degradation due to migration between electrodes and side reactions at the anode. Solid-state and hybrid electrolytes offer solutions but face challenges with ionic conductivity and interfacial stability. Achieving a stable electrolyte-electrode interface is critical, as liquid systems degrade the SEI over time, and solid-state interfaces suffer from mechanical stresses and high resistance. Liquid electrolytes also promote lithium dendrite growth, leading to safety issues, while solid-state systems resist penetration but still struggle with dendrite formation. Limited ionic conductivity in solid-state electrolytes at room temperature hinders rate capability and energy density, requiring advancements in ion transport pathways. High-concentration electrolytes improve SEI stability but suffer from high viscosity, which reduces ionic mobility, and high production costs, limiting their commercial potential.^{3,16,18,182,183}

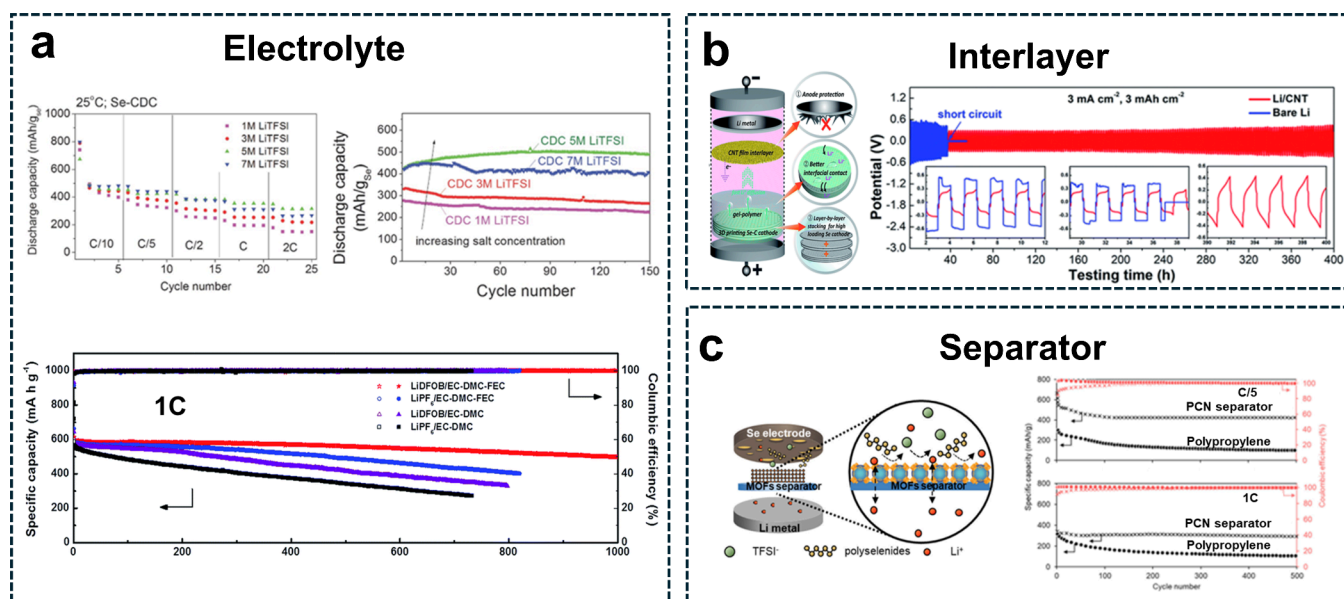


Figure 4. Alkali metal anode design. (a) (Top) Cycling performance with high concentration electrolyte (5 M LiTFSI in DME:DOL (1:1, vol.) with 0.2 M LiNO_3 .¹⁸⁴ (Reproduced with permission from ref 184. Copyright 2014, John Wiley and Sons.) (Bottom) Cycling performance and Coulombic efficiency of Li–Se cells using different electrolytes at 1C.¹¹⁵ (Reproduced with permission from ref 115. Copyright 2012, Royal Society of Chemistry) (b) (Top-left) Galvanostatic discharge/charge voltage profiles of CNT/Li electrodes in symmetric coin cells at a current density of 3 mA cm^{-2} and capacity loading of 3 mAh cm^{-2} for 400 cycles. Electrochemical performance of quasi-solid-state lithium–selenium batteries (QSSLSEBs) with gel polymer electrolytes (GPEs) employing the CNT interlayer at a current density of 1 mA cm^{-2} . (Top-right) Schematic illustration of a QSSLSEBs model.¹⁹⁹ (Reproduced with permission from ref 199. Copyright 2012, Royal Society of Chemistry) (c) Scheme illustrating a cation-selective PCN separator of PCN-250(Fe) metal–organic frameworks coated on a porous polypropylene membrane for suppressing polyselenides shuttle in Li/Se battery systems (Left). Electrochemical performance (rate and cycling) of Li/Se cells with a PCN separator (Right).⁴² (Reproduced with permission from ref 42. Copyright 2021, American Chemical Society.)

NEGATIVE ELECTRODE

Anode Materials Modifications and Strategies for Dendrite Suppression. Alkali metal–Se batteries generally employ alkali metals (such as Li, Na, and K) as anodes because of their high theoretical capacities compared to nonmetallic anodes.^{29,30,184,185} However, Se metal batteries face significant challenges on the anode side, such as dendritic growth on the metal surfaces during cycling and high electrochemical reactivity. These issues are critical for safety and can cause thermal run-away. In addition, the depletion of electrolytes and side reactions between the metal anode and electrolytes leads to poor safety, low Coulombic efficiency, and capacity fading.^{186–188} Various strategies have been proposed to address these problems, including electrolyte design, solid-state electrolytes, and construction of interlayers and host materials. In 2015, Lee et al. initiated a study on metal anode protection in Li–Se batteries using a high-concentration electrolyte.¹⁸⁴ They demonstrated that the formation of a LiF-rich solid electrolyte interface (SEI) layer increased the mechanical strength¹⁸⁹ using an electrolyte composed of 5 M LiTFSI dissolved in DME:DOL(1:1 volume ratio). The SEI layer exhibited higher ionic conductivity, resulting in a capacity retention of $\sim 99.9\%$ of the initial capacity after 150 cycles in the full Li–Se cell, Figure 4a and Figure S4 in SI section.^{30,115,184} LiNO_3 salt is commonly used as an additive to create a robust SEI layer with high ionic conductivity, suppressing dendrite growth in Li-metal batteries.^{190–195} Many studies on Li–Se batteries have suggested modifying electrolytes with LiNO_3 additives to improve the electrochemical performance.^{29,196}

High-concentration electrolytes have also shown promise in suppressing dendrite formation by promoting the formation of a stable, LiF-rich solid electrolyte interphase (SEI) layer on the anode. In systems with concentrated salts, such as LiTFSI in ether-based solvents, the SEI layer becomes more uniform and dense, which helps stabilize lithium deposition and minimize dendrite growth. This strategy also reduces solvent reactivity with lithium, resulting in improved cycle life and reduced capacity fade. However, increased electrolyte viscosity and higher costs are potential drawbacks of this approach, as discussed in recent studies.^{53,162} Interlayers, including carbon-based structures, lithiophilic coatings, and polymeric films, offer another effective strategy by acting as scaffolds that guide uniform lithium deposition across the anode surface, thereby preventing dendritic growth. Interlayers such as carbon nanotubes (CNTs) and lithiophilic ZnO coatings provide nucleation sites that promote even lithium distribution, reducing localized current density—a primary factor in dendrite formation. Comparative studies indicate that interlayers can achieve more stable cycling performance than high-concentration electrolytes alone. However, the complexity of interlayer integration and the potential increase in internal cell resistance remain challenges.^{92,144}

The high theoretical capacity and low electrochemical potential make Li metal the most widely used anode material for high-energy batteries. Consequently, most Li–Se studies employ Li metal as anodes. Integrating Sn-alloys based electrode in Se-systems using solid state electrolyte could prevent dendrite propagation, further enhancing battery safety and longevity.¹⁰⁷ Thus, a hybrid approach that combines high-concentration electrolytes with interlayers leverages the

benefits of both strategies, providing a robust SEI layer through the electrolyte while also guiding lithium deposition via the interlayer scaffold. Such configurations have demonstrated enhanced cycle life and stability, with studies showing that these hybrid systems achieve some of the best results for dendrite suppression and cycling efficiency to date. This comparative analysis emphasizes the effectiveness of different dendrite suppression strategies, providing insights into their respective advantages and limitations. The addition of interlayers, high-concentration electrolytes, or their combination represents a promising pathway to improve cycle life and safety in alkali metal batteries. Liu et al. suggested hybrid electrolytes combining liquid and solid phases to mitigate dendrite growth. This approach leverages the advantages of solid electrolytes^{197–199} and SEI layers formed from liquid electrolytes using a LiNO₃ additive, Figure 4a.

However, LiNO₃ has low solubility in carbonate-based electrolytes, limiting its use primarily to ether-based electrolytes.²⁰⁰ For carbonate-based electrolytes, highly soluble fluoroethylene carbonate (FEC)^{201–203} solvents are employed as additives to create inorganic LiF-rich SEI layers, Figure 4a. Zhou et al. introduced a novel electrolyte combining FEC solvent with LiDFOB salt to obtain a thin and dense SEI layer.¹¹⁵ This FEC-containing electrolyte transformed the fibrous morphology of deposited Li ions into small spherical particles during electrodeposition, resulting in a superior capacity of 511 mAh g⁻¹ after 1,000 cycles at a high 5C rate. This FEC-containing electrolyte transformed the fibrous morphology of deposited Li ions into small spherical particles during electrodeposition, resulting in a superior capacity of 511 mAh g⁻¹ after 1,000 cycles at a high 5C rate.

Artificial SEI Layer Formation. In addition to liquid electrolytes, Guo's group introduced in situ gelation in Li–Se batteries for the first time, utilizing the cationic ring-opening polymerization principle.²⁰⁴ Polymerization, generated from an electrochemical reaction between the 1,3-Dioxolane (DOL) solvent and the LiPF₆ salt, transformed the liquid electrolytes into gel polymers during cycling. These gelation electrolytes, deposited on the Li metal surface, restrained the side reactions between the Li metal and the electrolytes, improving capacity retention to 80%, compared to 60% retention in liquid electrolytes.

Li–Se batteries have been developed using various electrolytes, such as polymers, sulfides, oxide solid electrolytes, and liquid electrolytes.^{168,205,206} Lee's group presented a “one cathode design” cell, combining a cathode with polymer electrolytes electrodeposited on it to simultaneously control the shuttle effect and dendrite formation.²⁰⁵ Despite the promising properties of these materials, challenges remain, particularly in terms of their poor mechanical strength and inability to effectively suppress Li dendrite growth at high Se loadings and current densities.^{207,208} Recently, Gao et al. reported that a 3D-printed interlayer could inhibit dendrite growth, Figure 4b.¹⁹⁹ Symmetric cell tests demonstrated the effectiveness of the constructed interlayer in suppressing dendritic growth.¹⁹⁹ Sathitsuksanoh et al. proposed a separator coated with MOF to fix Lewis base sites, enabling reversible plating/stripping behavior, Figure 4c. This approach blocks the TFSI⁻ anion, a Lewis base from reaching the anode side selectively interacting with the separator surface during cycling. This mechanism promotes stable and uniform Li electro-deposition on the Li metal anode, achieving a high Li⁺ transference number.⁴² Na-metal anodes are also being

explored due to the abundance and high specific capacity (~1,166 mA h g⁻¹) of Na. However, challenges such as surface instability, dendritic growth, and volumetric changes have hindered the commercialization of Na–Se batteries.²⁰⁹ Hu et al. suggested a dendrite-free anode with strong sodiophilic properties, derived from an N,O-codoped carbon host using a Zn-based MOF (denoted NOC/Na). The NOC/Na host exhibited higher ionic conductivity, providing more Na⁺ deposition sites for uniform plating and reducing the effective current density, which in turn stabilized the Na metal during cycling.²¹⁰ The NOC/Na structure mitigated dendritic growth during cycling, and the full cell incorporating a Ni-SA/NOC cathode, retained a capacity of 213 mAh g⁻¹ (1026 mAh cm⁻³) even after 1,000 cycles at 1C rate.

Future research should focus on optimizing the interactions between the electrodes and electrolytes, further developing hybrid electrolytes that combine liquid and solid-state benefits to enhance ionic conductivity and safety, addressing SEI formation and growth, further exploring Na and K as viable and cost-effective anodes.

Song et al. demonstrated that the copresence of Py_{1,4}TFSI and LiNO₃ in the electrolyte can protect the lithium anode by forming a stable solid electrolyte interphase (SEI) rich in LiF, LiN_xO_y, and conductive Li₃N. This smooth SEI minimizes morphological changes to the lithium anode during cycling, effectively mitigating lithium dendrite growth and undesirable side reactions with soluble cathode intermediates.²¹¹ The concept of bilayer artificial SEI (BL-SEI) introduced by Zhang's group highlights the potential of combining graphitic layers (GLs) with inorganic layers (ILs) such as LiF and Li₂CO₃ to enhance lithium metal anode stability. The GLs provide high mechanical strength, mitigating stress from nonuniform lithium deposition, while the ILs prevent corrosion from the electrolyte. DFT-based charge density difference analysis, Figure S5a-d SI section, and stress–strain evaluations, Figure S5e-h SI section, further reveal the stability, ionic conductivity, and mechanical resilience of the graphene/LiF <111> BL-SEI, positioning it as promising artificial SEI candidate. Expanding on this theoretical framework, future studies could explore the design of artificial SEIs for selenium batteries.²¹²

Alkali metals are preferred as anodes in Se batteries owing to their high theoretical capacities compared to other anode materials, such as graphite and hard carbon. Nonmetallic anodes require an additional lithiation step and still exhibit lower energy densities than alkali metal anodes.^{213,214} For example, Si anodes in Se batteries undergoes significant volume changes—up to 400%—during lithiation and delithiation, which can hinder the capacity and long-term cycling stability of Se batteries.¹⁸⁵ While alkali metals offer advantages in terms of energy density, their use as anodes in Se batteries poses challenges, including electrolyte depletion, volume expansion, and dendrite formation during charge/discharge cycles.

In summary, this review explores the key advancements and persistent challenges in the development of Se alkali metal batteries, including redox mechanisms, electrode designs, and electrolytic configurations. Innovative cathode materials such as conductive porous carbon hosts, MoFs, and conductive polymers have shown improved performance and stability by mitigating issues such as polyselenide dissolution and shuttle effects. On the anode side, despite the high theoretical capacities of alkali metals (Li, Na, and K), challenges such as dendrite formation, electrolyte depletion, and volume changes remain. Strategies such as high-concentration electrolytes, solid-state electrolytes, and protective interlayers have demonstrated the potential for enhancing anode stability.

Table S2 in SI section reports visual understanding of the advantages and limitations of each alkali metal–selenium system discussed and highlights the specific challenges each one faces. The included table presents these performance differences across various parameters, such as energy density, cycle stability, and reaction kinetics. This comparative approach underscores why, despite their inherent advantages, each alkali metal–selenium system encounters unique challenges that must be addressed in the future to enhance their practical applications. Future research should focus on optimizing the interactions between the electrodes and electrolytes, further developing hybrid electrolytes that combine liquid and solid-state benefits to enhance ionic conductivity and safety, addressing SEI formation and growth, further exploring Na and K as viable and cost-effective anodes. Advanced electrode design by developing 3D-structured or porous materials to improve electronic conductivity and accommodate volume changes for better cycling stability should be explored. Integrating individual strategies for dendrite suppression, including high concentration electrolytes and interlayer design should address challenges on practical applications, i.e. high loading and long cycling. Sustainability exploring the recycling and reuse of waste materials should be improved. These approaches could lead to more sustainable and commercially viable Se-based batteries. In conclusion, although significant progress has been made, continued innovation in material engineering and electrolyte formulation is crucial to fully leverage the potential of Se-alkali metal batteries. Addressing the remaining challenges could make these batteries key technologies for high-performance and sustainable energy storage.

■ ASSOCIATED CONTENT

SI Supporting Information

The Supporting Information is available free of charge at <https://pubs.acs.org/doi/10.1021/acsenerylett.5c00768>.

DFT calculation; binding energy; energy plot; voltage curves; schematic of manufacturing Se-composite; HR-TEM/EDX; LUMO energy level; cycle performance; electrode potential; charge density; comparison of advantages and disadvantages of different electrolyte systems for Se batteries; comparison of alkaline Se systems in terms of theoretical capacity, cycle-life, polyselenide solubility, diffusion coefficient and redox kinetics (PDF)

■ AUTHOR INFORMATION

Corresponding Authors

Marco Agostini – Department of Chemistry and Drug Technologies, “Sapienza” University of Rome, 00185 Rome, Italy; orcid.org/0000-0002-4152-8894;

Email: marco.agostini@uniroma1.it

Jang-Yeon Hwang – Department of Energy Engineering, Hanyang University, Seoul 04763, Republic of Korea; Department of Battery Engineering, Hanyang University, Seoul 04763, Republic of Korea; orcid.org/0000-0003-3802-7439; Email: jangyeonhw@hanyang.ac.kr

Authors

Jimin Park – Department of Energy Engineering, Hanyang University, Seoul 04763, Republic of Korea

Hyerim Kim – Department of Energy Engineering, Hanyang University, Seoul 04763, Republic of Korea

Arcangelo Celeste – Department of Chemistry, “Sapienza” University of Rome, 00185 Rome, Italy; orcid.org/0000-0002-3421-2322

Hyeona Park – Department of Energy Engineering, Hanyang University, Seoul 04763, Republic of Korea

Shivam Kansara – Department of Energy Engineering, Hanyang University, Seoul 04763, Republic of Korea; orcid.org/0000-0003-0908-8267

Rosaceleste Zumpano – Department of Chemistry and Drug Technologies, “Sapienza” University of Rome, 00185 Rome, Italy

Vanessa Piacentini – Department of Chemistry, “Sapienza” University of Rome, 00185 Rome, Italy

Sergio Brutti – Department of Chemistry, “Sapienza” University of Rome, 00185 Rome, Italy; orcid.org/0000-0001-8853-9710

Aleksandar Matic – Department of Physics, Chalmers University of Technology, 41296 Göteborg, Sweden; orcid.org/0000-0003-4414-9504

Complete contact information is available at:

<https://pubs.acs.org/doi/10.1021/acsenerylett.5c00768>

Author Contributions

#J.P., H.K., and A.C. contributed equally to this work.

Notes

The authors declare no competing financial interest.

Biographies

Jimin Park is presently a Ph.D. candidate under the supervision of Prof. Jang-Yeon Hwang in the Department of Energy Engineering at Hanyang University, Republic of Korea. Her current research interests focus on the design and synthesis of functionalized cathode materials and electrolyte design for alkali-ion and alkali-metal batteries.

Hyerim Kim is presently a Ph.D. candidate under the supervision of Prof. Jang-Yeon Hwang in the Department of Energy Engineering at Hanyang University, Republic of Korea. Her current research interests focus on the design of electrode and electrolyte materials for alkali-metal batteries.

Arcangelo Celeste received his Ph.D. degree (2022) from University of Genoa, Italy. He is currently an assistant professor at Sapienza University of Rome, Italy, working on developing new electrodes for applications in rechargeable alkali-metal batteries.

Hyeona Park is presently a Ph.D. candidate under the supervision of Prof. Jang-Yeon Hwang in the Department of Energy Engineering at Hanyang University, Republic of Korea. She focused on developing

performance of lithium–sulfur batteries with high loading sulfur cathode, electrolyte modulation, and stabilization of Li-metal anode.

Shivam Kansara received his Ph.D. degree (2019) from Sardar Vallabhbhai National Institute of Technology (SVNIT), India. He is currently a postdoctoral researcher at the department of energy engineering Hanyang University, South Korea, focusing on fundamental mechanisms governing the behaviors of materials in batteries systems, involving quantum mechanics.

Rosaceleste Zumpano received her Ph.D. degree (2020) from Sapienza University of Rome, Italy. She is currently a postdoctoral researcher at Sapienza University of Rome, Italy, focusing on developing nanostructured materials for applications in biosensors.

Vanessa Piacentini is presently a Ph.D. candidate from Sapienza University of Rome, Italy. Her research focus on computational methods applied to electrolytes development for applications in rechargeable batteries.

Sergio Brutti is currently an associated professor in Physical Chemistry at Sapienza University of Rome, Italy. His research interests fall in the field of solid state chemistry and thermodynamics with the aim to develop advanced materials for energy applications.

Aleksandar Matic is a Professor in the Department of Physics at Chalmers University of Technology, Sweden, and leads the Division of Materials Physics. He is also leading the strategic initiative in research and education for battery technology. His research focuses on next-generation batteries, particularly metal anodes and operando characterization.

Marco Agostini received his Ph.D. in Materials Science (2014) at Sapienza University of Rome, Italy under Prof. Bruno Scrosati. He worked at Chalmers University of Technology (2016–2020) and, since 2022, has been a tenure-track researcher at Sapienza University of Rome, focusing on rechargeable alkali-metal batteries.

Jang-Yeon Hwang received his Ph.D. degree (2018) at Hanyang University, Republic of Korea. He is an Associate Professor in the Department of Energy Engineering & Battery Engineering at Hanyang University. His research is focused on the development of novel electrode materials for the high-energy alkali-ion, alkali-metal, and sulfur batteries.

ACKNOWLEDGMENTS

The contribution of S.B. and A.C. to this study was carried out within the NEST—Network for Energy Sustainable Transition and received funding from the European Union Next-Generation EU (PIANO NAZIONALE DI RIPRESA E RESILIENZA (PNRR)—MISSIONE 4 COMPONENTE 2, INVESTIMENTO 1.3—D.D. 1561 11/10/2022, B53C22004070006). This manuscript reflects only the authors' views and opinions, neither the European Union nor the European Commission can be considered responsible for them. All Sapienza staff within the NEST project participate in this action under the frame of the grant PE2421852F05911E. This work was supported by a National Research Foundation of Korea (NRF) grant funded by the Government of the Republic of Korea (Ministry of Science and ICT, RS-2024-00449682 and RS-2024-00455177).

REFERENCES

- (1) Abouimrane, A.; Dambournet, D.; Chapman, K. W.; Chupas, P. J.; Weng, W.; Amine, K. A New Class of Lithium and Sodium Rechargeable Batteries Based on Selenium and Selenium-Sulfur as a Positive Electrode. *J. Am. Chem. Soc.* **2012**, *134* (10), 4505–4508.
- (2) Cui, Y.; Abouimrane, A.; Lu, J.; Bolin, T.; Ren, Y.; Weng, W.; Sun, C.; Maroni, V. A.; Heald, S. M.; Amine, K. (De)Lithiation Mechanism of Li/SeS_x (x = 0–7) Batteries Determined by in Situ Synchrotron x-Ray Diffraction and X-Ray Absorption Spectroscopy. *J. Am. Chem. Soc.* **2013**, *135* (21), 8047–8056.
- (3) Luo, C.; Xu, Y.; Zhu, Y.; Liu, Y.; Zheng, S.; Liu, Y.; Langrock, A.; Wang, C. Selenium@Mesoporous Carbon Composite with Superior Lithium and Sodium Storage Capacity. *ACS Nano* **2013**, *7* (9), 8003–8010.
- (4) Huang, H.; Xu, R.; Feng, Y.; Zeng, S.; Jiang, Y.; Wang, H.; Luo, W.; Yu, Y. Sodium/Potassium-Ion Batteries: Boosting the Rate Capability and Cycle Life by Combining Morphology, Defect and Structure Engineering. *Adv. Mater.* **2020**, *32* (8), 1904320.
- (5) Luo, C.; Zhu, Y.; Wen, Y.; Wang, J.; Wang, C. Carbonized Polyacrylonitrile-Stabilized SeS_x Cathodes for Long Cycle Life and High Power Density Lithium Ion Batteries. *Adv. Funct. Mater.* **2014**, *24* (26), 4082–4089.
- (6) Papp, J. F. *Mineral Commodity Summaries* 2023; **2023**.
- (7) Wan, H.; Liu, G.; Li, Y.; Weng, W.; Mwizerwa, J. P.; Tian, Z.; Chen, L.; Yao, X. Transitional Metal Catalytic Pyrite Cathode Enables Ultrastable Four-Electron-Based All-Solid-State Lithium Batteries. *ACS Nano* **2019**, *13* (8), 9551–9560.
- (8) Tian, F.; Chang, M.; Yang, M.; Xie, W.; Chen, S.; Yao, X. Multi-Electron Reaction Based Molybdenum Pentasulfide towards High-Energy Density All-Solid-State Lithium Batteries. *Chem. Eng. J.* **2023**, *472*, 144914.
- (9) Liu, G.; Yang, J.; Wu, J.; Peng, Z.; Yao, X. Inorganic Sodium Solid Electrolytes: Structure Design, Interface Engineering and Application. *Adv. Mater.* **2024**, *36*, 2311475.
- (10) Wu, J.; Liu, S.; Han, F.; Yao, X.; Wang, C. Lithium/Sulfide All-Solid-State Batteries Using Sulfide Electrolytes. *Adv. Mater.* **2021**, *33*, 2000751.
- (11) Yang, M.; Yao, Y.; Chang, M.; Tian, F.; Xie, W.; Zhao, X.; Yu, Y.; Yao, X. High Energy Density Sulfur-Rich MoS₆-Based Nanocomposite for Room Temperature All-Solid-State Lithium Metal Batteries. *Adv. Energy Mater.* **2023**, *13* (28), 2300962.
- (12) Sun, J.; Du, Z.; Liu, Y.; Ai, W.; Wang, K.; Wang, T.; Du, H.; Liu, L.; Huang, W. State-Of-The-Art and Future Challenges in High Energy Lithium-Selenium Batteries. *Adv. Mater.* **2021**, *33*, 2003845.
- (13) Zhang, Z.; Zhang, Z.; Zhang, K.; Yang, X.; Li, Q. Improvement of Electrochemical Performance of Rechargeable Lithium-Selenium Batteries by Inserting a Free-Standing Carbon Interlayer. *RSC Adv.* **2014**, *4* (30), 15489–15492.
- (14) Cui, Y.; Abouimrane, A.; Sun, C. J.; Ren, Y.; Amine, K. Li-Se Battery: Absence of Lithium Polyselenides in Carbonate Based Electrolyte. *Chem. Commun.* **2014**, *50* (42), 5576–5579.
- (15) Ye, H.; Yin, Y. X.; Zhang, S. F.; Guo, Y. G. Advanced Se-C Nanocomposites: A Bifunctional Electrode Material for Both Li-Se and Li-Ion Batteries. *J. Mater. Chem. A Mater.* **2014**, *2* (33), 13293–13298.
- (16) Li, Z.; Yuan, L.; Yi, Z.; Liu, Y.; Huang, Y. Confined Selenium within Porous Carbon Nanospheres as Cathode for Advanced Li-Se Batteries. *Nano Energy* **2014**, *9*, 229–236.
- (17) Lai, Y.; Yang, F.; Zhang, Z.; Jiang, S.; Li, J. Encapsulation of Selenium in Porous Hollow Carbon Spheres for Advanced Lithium-Selenium Batteries. *RSC Adv.* **2014**, *4* (74), 39312–39315.
- (18) Zhang, J.; Zhang, Z.; Li, Q.; Qu, Y.; Jiang, S. Selenium Encapsulated into Interconnected Polymer-Derived Porous Carbon Nanofiber Webs as Cathode Materials for Lithium-Selenium Batteries. *J. Electrochem. Soc.* **2014**, *161* (14), A2093–A2098.
- (19) Wang, H.; Li, S.; Chen, Z.; Liu, H. K.; Guo, Z. A Novel Type of One-Dimensional Organic Selenium-Containing Fiber with Superior Performance for Lithium-Selenium and Sodium-Selenium Batteries. *RSC Adv.* **2014**, *4* (106), 61673–61678.
- (20) Gates, B.; Yin, Y.; Xia, Y. A Solution-Phase Approach to the Synthesis of Uniform Nanowires of Crystalline Selenium with Lateral Dimensions in the Range of 10–30 nm. *J. Am. Chem. Soc.* **2000**, *122* (50), 12582–12583.

- (21) Liu, H.; Wang, L.; Xiao, X.; De Carlo, F.; Feng, J.; Mao, H.; Hemley, R. J. Anomalous High-Pressure Behavior of Amorphous Selenium from Synchrotron x-Ray Diffraction and Microtomography. *P. NATL. ACAD. SCI. USA* **2008**, *105* (36), 13229–13234.
- (22) Shportko, K.; Kremers, S.; Woda, M.; Lencer, D.; Robertson, J.; Wuttig, M. Resonant Bonding in Crystalline Phase-Change Materials. *Nat. Mater.* **2008**, *7* (8), 653–658.
- (23) Zhou, X.; Gao, P.; Sun, S.; Bao, D.; Wang, Y.; Li, X.; Wu, T.; Chen, Y.; Yang, P. Amorphous, Crystalline and Crystalline/Amorphous Selenium Nanowires and Their Different (De)Lithiation Mechanisms. *Chem. Mater.* **2015**, *27* (19), 6730–6736.
- (24) Qu, Y.; Zhang, Z.; Lai, Y.; Liu, Y.; Li, J. A Bimodal Porous Carbon with High Surface Area Supported Selenium Cathode for Advanced Li-Se Batteries. *Solid State Ionics* **2015**, *274*, 71–76.
- (25) Zhang, Z.; Yang, X.; Guo, Z.; Qu, Y.; Li, J.; Lai, Y. Selenium/Carbon-Rich Core-Shell Composites as Cathode Materials for Rechargeable Lithium-Selenium Batteries. *J. Power Sources* **2015**, *279*, 88–93.
- (26) Yi, Z.; Yuan, L.; Sun, D.; Li, Z.; Wu, C.; Yang, W.; Wen, Y.; Shan, B.; Huang, Y. High-Performance Lithium-Selenium Batteries Promoted by Heteroatom-Doped Microporous Carbon. *J. Mater. Chem. A* **2015**, *3* (6), 3059–3065.
- (27) Yang, C. P.; Yin, Y. X.; Guo, Y. G. Elemental Selenium for Electrochemical Energy Storage. *J. Phys. Chem. Lett.* **2015**, *6* (2), 256–266.
- (28) Youn, H. C.; Jeong, J. H.; Roh, K. C.; Kim, K. B. Graphene-Selenium Hybrid Microballs as Cathode Materials for High-Performance Lithium-Selenium Secondary Battery Applications. *Sci. Rep.* **2016**, *6*, 30865 DOI: 10.1038/srep30865.
- (29) Huang, D.; Li, S.; Luo, Y.; Xiao, X.; Gao, L.; Wang, M.; Shen, Y. Graphene Oxide-Protected Three Dimensional Se as a Binder-Free Cathode for Li-Se Battery. *Electrochim. Acta* **2016**, *190*, 258–263.
- (30) Zhou, Y.; Li, Z.; Lu, Y. C. A Stable Lithium-Selenium Interface via Solid/Liquid Hybrid Electrolytes: Blocking Polyselenides and Suppressing Lithium Dendrite. *Nano Energy* **2017**, *39*, 554–561.
- (31) Xu, G. L.; Liu, J.; Amine, R.; Chen, Z.; Amine, K. Selenium and Selenium-Sulfur Chemistry for Rechargeable Lithium Batteries: Interplay of Cathode Structures, Electrolytes, and Interfaces. *ACS Energy Lett.* **2017**, *2* (3), 605–614.
- (32) Eftekhari, A. The Rise of Lithium-Selenium Batteries. *Sustain. Energy Fuels* **2017**, *1*, 14–29.
- (33) Mukkablal, R.; Deshagani, S.; Deepa, M.; Shivaprasad, S. M.; Ghosal, P. Carbon Black Free Selenium/CTAB Decorated Carbon Nanotubes Composite with High Selenium Content for Li-Se Batteries. *Electrochim. Acta* **2018**, *283*, 63–74.
- (34) Mukkablal, R.; Kuldeep; Killi, K.; Shivaprasad, S. M.; Deepa, M. Metal Oxide Interlayer for Long-Lived Lithium-Selenium Batteries. *Chem.—Eur. J.* **2018**, *24* (65), 17327–17338.
- (35) Kim, W.; Lee, J.; Lee, S.; Eom, K. S.; Pak, C.; Kim, H. J. Advanced Ordered Mesoporous Carbon with Fast Li-Ion Diffusion for Lithium-Selenium Sulfide Batteries in a Carbonate-Based Electrolyte. *Carbon* **2020**, *170*, 236–244.
- (36) Wang, Y.; Liang, P.; Yang, H.; Li, W.; Wang, Z.; Liu, Z.; Wang, J.; Shen, X. Hollow CoP Nanoparticles Embedded in Two-Dimensional N-Doped Carbon Arrays Enabling Advanced Li-SeS₂ Batteries with Rapid Kinetics. *Mater. Today Energy* **2020**, *17*, 100423.
- (37) Li, H.; Dong, W.; Li, C.; Barakat, T.; Sun, M.; Wang, Y.; Wu, L.; Wang, L.; Xia, L.; Hu, Z. Y.; Li, Y.; Su, B. L. Three-Dimensional Ordered Hierarchically Porous Carbon Materials for High Performance Li-Se Battery. *J. Energy Chem.* **2022**, *68*, 624–636.
- (38) Wu, C.; Yuan, L.; Li, Z.; Yi, Z.; Zeng, R.; Li, Y.; Huang, Y. High-Performance Lithium-Selenium Battery with Se/Microporous Carbon Composite Cathode and Carbonate-Based Electrolyte. *Sci. China Mater.* **2015**, *58* (2), 91–97.
- (39) Mutlu, T.; Demir-Cakan, R. Carbonate or Ether Based Electrolyte for Li-Se Batteries: An in-Situ Study of Intermediate Polyselenide Formation. *Electrochim. Acta* **2021**, *390*, 138825.
- (40) Luo, C.; Wang, J.; Suo, L.; Mao, J.; Fan, X.; Wang, C. In Situ Formed Carbon Bonded and Encapsulated Selenium Composites for Li-Se and Na-Se Batteries. *J. Mater. Chem. A Mater.* **2015**, *3* (2), 555–561.
- (41) Mukkablal, R.; Kuldeep; Deepa, M. Poly(Carbazole)-Coated Selenium@Conical Carbon Nanofibers Hybrid for Lithium-Selenium Batteries with Enhanced Lifespan. *ACS Appl. Energy Mater.* **2018**, *1* (12), 6964–6976.
- (42) Hossain, M. A.; Tulaphol, S.; Thapa, A. K.; Rahaman, M. S.; Jasinski, J. B.; Wang, H.; Sunkara, M. K.; Syzdek, J.; Ozdemir, O. K.; Ornstein, J. M.; Sathitsuksanoh, N. Metal-Organic Framework Separator as a Polyselenide Filter for High-Performance Lithium-Selenium Batteries. *ACS Appl. Energy Mater.* **2021**, *4* (12), 13450–13460.
- (43) Wu, F.; Lee, J. T.; Xiao, Y.; Yushin, G. Nanostructured Li₂Se Cathodes for High Performance Lithium-Selenium Batteries. *Nano Energy* **2016**, *27*, 238–246.
- (44) Li, X.; Liang, J.; Kim, J. T.; Fu, J.; Duan, H.; Chen, N.; Li, R.; Zhao, S.; Wang, J.; Huang, H.; Sun, X. Highly Stable Halide-Electrolyte-Based All-Solid-State Li-Se Batteries. *Adv. Mater.* **2022**, *34* (20), 2200856 DOI: 10.1002/adma.202200856.
- (45) Huang, Y.; Lin, L.; Zhang, C.; Liu, L.; Li, Y.; Qiao, Z.; Lin, J.; Wei, Q.; Wang, L.; Xie, Q.; Peng, D. L. Recent Advances and Strategies toward Polysulfides Shuttle Inhibition for High-Performance Li-S Batteries. *Adv. Sci.* **2022**, *9*, 2106004.
- (46) Yang, S.; Zhang, Z.; Lin, J.; Zhang, L.; Wang, L.; Chen, S.; Zhang, C.; Liu, X. Recent Progress in Quasi-/All-Solid-State Electrolytes for Lithium-Sulfur Batteries. *Front. Energy Res.* **2022**, *10*, 945003 DOI: 10.3389/fenrg.2022.945003.
- (47) Zhang, Q.; Wan, H.; Liu, G.; Ding, Z.; Mwiszerwa, J. P.; Yao, X. Rational Design of Multi-Channel Continuous Electronic/Ionic Conductive Networks for Room Temperature Vanadium Tetrasulfide-Based All-Solid-State Lithium-Sulfur Batteries. *Nano Energy* **2019**, *57*, 771–782.
- (48) Wan, H.; Cai, L.; Yao, Y.; Weng, W.; Feng, Y.; Mwiszerwa, J. P.; Liu, G.; Yu, Y.; Yao, X. Self-Formed Electronic/Ionic Conductive Fe₃S₄@S@0.9Na₃SbS₄-0.1NaI Composite for High-Performance Room-Temperature All-Solid-State Sodium-Sulfur Battery. *Small* **2020**, *16* (34), 2001574.
- (49) Chen, S.; Xie, D.; Liu, G.; Mwiszerwa, J. P.; Zhang, Q.; Zhao, Y.; Xu, X.; Yao, X. Sulfide Solid Electrolytes for All-Solid-State Lithium Batteries: Structure, Conductivity, Stability and Application. *Energy Storage Mater.* **2018**, *14*, 58–74.
- (50) Shi, J.; Liu, G.; Weng, W.; Cai, L.; Zhang, Q.; Wu, J.; Xu, X.; Yao, X. Co₃S₄@Li₂P₃S₁₁ Hexagonal Platelets as Cathodes with Superior Interfacial Contact for All-Solid-State Lithium Batteries. *ACS Appl. Mater. Interfaces* **2020**, *12* (12), 14079–14086.
- (51) Li, Q.; Liu, H.; Yao, Z.; Cheng, J.; Li, T.; Li, Y.; Wolverton, C.; Wu, J.; Druvid, V. P. Electrochemistry of Selenium with Sodium and Lithium: Kinetics and Reaction Mechanism. *ACS Nano* **2016**, *10* (9), 8788–8795.
- (52) Xu, Q.; Liu, T.; Li, Y.; Hu, L.; Dai, C.; Zhang, Y.; Li, Y.; Liu, D.; Xu, M. Selenium Encapsulated into Metal-Organic Frameworks Derived N-Doped Porous Carbon Polyhedrons as Cathode for Na-Se Batteries. *ACS Appl. Mater. Interfaces* **2017**, *9* (47), 41339–41346.
- (53) Ding, J.; Zhou, H.; Zhang, H.; Stephenson, T.; Li, Z.; Karpuzov, D.; Mitlin, D. Exceptional Energy and New Insight with a Sodium-Selenium Battery Based on a Carbon Nanosheet Cathode and a Pseudographite Anode. *Energy Environ. Sci.* **2017**, *10* (1), 153–165.
- (54) Yuan, B.; Sun, X.; Zeng, L.; Yu, Y.; Wang, Q. A Freestanding and Long-Life Sodium-Selenium Cathode by Encapsulation of Selenium into Microporous Multichannel Carbon Nanofibers. *Small* **2018**, *14* (9), 1703252.
- (55) Yang, X.; Wang, J.; Wang, S.; Wang, H.; Tomanec, O.; Zhi, C.; Zboril, R.; Yu, D. Y. W.; Rogach, A. Vapor-Infiltration Approach toward Selenium/Reduced Graphene Oxide Composites Enabling Stable and High-Capacity Sodium Storage. *ACS Nano* **2018**, *12* (7), 7397–7405.
- (56) Kang, Y. C.; Kim, J. K. Encapsulation of Se into Hierarchically Porous Carbon Microspheres with Optimized Pore Structure for

- Advanced Na-Se and K-Se Batteries. *ACS Nano* **2020**, *14* (10), 13203–13216.
- (57) Perras, F. A.; Hwang, S.; Wang, Y.; Self, E. C.; Liu, P.; Biswas, R.; Nagarajan, S.; Pham, V. H.; Xu, Y.; Boscoboinik, J. A.; Su, D.; Nanda, J.; Pruski, M.; Mitlin, D. Site-Specific Sodiation Mechanisms of Selenium in Microporous Carbon Host. *Nano Lett.* **2020**, *20* (2), 918–928.
- (58) Huang, X. L.; Zhou, C.; He, W.; Sun, S.; Chueh, Y. L.; Wang, Z. M.; Liu, H. K.; Dou, S. X. An Emerging Energy Storage System: Advanced Na-Se Batteries. *ACS Nano* **2021**, *15* (4), 5876–5903.
- (59) Wu, X.; Chen, X.; Wu, H.; Xie, B.; Wang, D.; Wang, R.; Zhang, X.; Piao, Y.; Diao, G.; Chen, M. Encapsulation of Se in Dual-Wall Hollow Carbon Spheres: Physical Confinement and Chemisorption for Superior Na-Se and K-Se Batteries. *Carbon* **2022**, *187*, 354–364.
- (60) Xiao, F.; Yang, X.; Yao, T.; Wang, H.; Rogach, A. L. Encapsulation of Selenium in MOF-Derived N,O-Codoped Porous Flower-like Carbon Host for Na-Se Batteries. *Chem. Eng. J.* **2022**, *430*, 132737.
- (61) Asif, M.; Ali, Z.; Ali, M.; Rashad, M. Investigating Role of Ammonia in Nitrogen-Doping and Suppressing Polyselenide Shuttle Effect in Na-Se Batteries. *J. Colloid Interface Sci.* **2022**, *617*, 641–650.
- (62) Wang, C.; Li, T.; Hou, X.; Jiang, M.; Zheng, Q.; Li, X. Rationally Designed Oxygen Vacancy for Achieving Effective and Kinetically Boosted Na-Se Batteries. *Chem. Eng. J.* **2023**, *451*, 139062.
- (63) Liu, Y.; Tai, Z.; Zhang, Q.; Wang, H.; Pang, W. K.; Liu, H. K.; Konstantinov, K.; Guo, Z. A New Energy Storage System: Rechargeable Potassium-Selenium Battery. *Nano Energy* **2017**, *35*, 36–43.
- (64) Yao, Y.; Xu, R.; Chen, M.; Cheng, X.; Zeng, S.; Li, D.; Zhou, X.; Wu, X.; Yu, Y. Encapsulation of Se₂ into Nitrogen-Doped Free-Standing Carbon Nanofiber Film Enabling Long Cycle Life and High Energy Density K-Se₂ Battery. *ACS Nano* **2019**, *13* (4), 4695–4704.
- (65) Huang, X.; Deng, J.; Qi, Y.; Liu, D.; Wu, Y.; Gao, W.; Zhong, W.; Zhang, F.; Bao, S.; Xu, M. A Highly-Effective Nitrogen-Doped Porous Carbon Sponge Electrode for Advanced K-Se Batteries. *Inorg. Chem. Front.* **2020**, *7* (5), 1182–1189.
- (66) Huang, X. L.; Guo, Z.; Dou, S. X.; Wang, Z. M. Rechargeable Potassium-Selenium Batteries. *Adv. Funct. Mater.* **2021**, *31*, 2102326.
- (67) Huang, X.; Sun, J.; Wang, L.; Tong, X.; Dou, S. X.; Wang, Z. M. Advanced High-Performance Potassium-Chalcogen (S, Se, Te) Batteries. *Small* **2021**, *17*, 2004369.
- (68) Ding, Y.; Cai, J.; Sun, Y.; Shi, Z.; Yi, Y.; Liu, B.; Sun, J. Bimetallic Selenide Decorated Nanoreactor Synergizing Confinement and Electrocatalysis of Se Species for 3D-Printed High-Loading K-Se Batteries. *ACS Nano* **2022**, *16* (2), 3373–3382.
- (69) Wang, H.; Wang, P.; Cao, J.; Liang, C.; Yu, K. N/S Co-Doped Biomass-Based Porous Carbon Surface-Embedded Small-Molecule Selenium as Cathode for High-Performance K-Se Batteries. *Electrochim. Acta* **2022**, *432* (10), 141158.
- (70) Yuan, Z.; Zeng, Z.; Zhao, W.; Dong, Y.; Lei, H.; Dong, Z.; Yang, Y.; Sun, W.; Ge, P. Recent Advances in Rechargeable Sodium-Selenium Batteries: A Mini Review. *J. Power Sources* **2024**, *602*, 234326.
- (71) Ding, J.; Wang, Y.; Huang, Z.; Song, W.; Zhong, C.; Ding, J.; Hu, W. Toward Theoretical Capacity and Superhigh Power Density for Potassium-Selenium Batteries via Facilitating Reversible Potassiation Kinetics. *ACS Appl. Mater. Interfaces* **2022**, *14* (5), 6828–6840.
- (72) Zhou, X.; Wang, L.; Yao, Y.; Jiang, Y.; Xu, R.; Wang, H.; Wu, X.; Yu, Y. Integrating Conductivity, Captivity, and Immobility Ability into N/O Dual-Doped Porous Carbon Nanocage Anchored with CNT as an Effective Se Host for Advanced K-Se Battery. *Adv. Funct. Mater.* **2020**, *30* (43), 2003871 DOI: 10.1002/adfm.202003871.
- (73) Yao, Y.; Chen, M.; Xu, R.; Zeng, S.; Yang, H.; Ye, S.; Liu, F.; Wu, X.; Yu, Y. CNT Interwoven Nitrogen and Oxygen Dual-Doped Porous Carbon Nanosheets as Free-Standing Electrodes for High-Performance Na-Se and K-Se Flexible Batteries. *Adv. Mater.* **2018**, *30* (49), 1805234.
- (74) Huang, X.; Xu, Q.; Gao, W.; Yang, T.; Zhan, R.; Deng, J.; Guo, B.; Tao, M.; Liu, H.; Xu, M. Rechargeable K-Se Batteries Based on Metal-Organic-Frameworks-Derived Porous Carbon Matrix Confined Selenium as Cathode Materials. *J. Colloid Interface Sci.* **2019**, *539*, 326–331.
- (75) Liu, Q.; Deng, W.; Pan, Y.; Sun, C. F. Approaching the Voltage and Energy Density Limits of Potassium-Selenium Battery Chemistry in a Concentrated Ether-Based Electrolyte. *Chem. Sci.* **2020**, *11* (23), 6045–6052.
- (76) Wei, C.; Song, J.; Wang, Y.; Tang, X.; Liu, X. Recent Development of Aqueous Multivalent-Ion Batteries Based on Conversion Chemistry. *Adv. Funct. Mater.* **2023**, *33*, 2304223.
- (77) Zhao-Karger, Z.; Lin, X. M.; Bonatto Minella, C.; Wang, D.; Diemant, T.; Behm, R. J.; Fichtner, M. Selenium and Selenium-Sulfur Cathode Materials for High-Energy Rechargeable Magnesium Batteries. *J. Power Sources* **2016**, *323*, 213–219.
- (78) Xu, J.; Wei, Z.; Zhang, S.; Wang, X.; Wang, Y.; He, M.; Huang, K. Hierarchical WSe₂ Nanoflower as a Cathode Material for Rechargeable Mg-Ion Batteries. *J. Colloid Interface Sci.* **2021**, *588*, 378–383.
- (79) Dai, C.; Hu, L.; Chen, H.; Jin, X.; Han, Y.; Wang, Y.; Li, X.; Zhang, X.; Song, L.; Xu, M.; Cheng, H.; Zhao, Y.; Zhang, Z.; Liu, F.; Qu, L. Enabling Fast-Charging Selenium-Based Aqueous Batteries via Conversion Reaction with Copper Ions. *Nat. Commun.* **2022**, *13* (1), 1863.
- (80) Zhang, J.; Zhang, X.; Xu, C.; Yan, H.; Liu, Y.; Xu, J.; Yu, H.; Zhang, L.; Shu, J. Four-Electron Transfer Reaction Endows High Capacity for Aqueous Cu-Se Battery. *Adv. Energy Mater.* **2022**, *12* (19), 2103998.
- (81) Lei, H.; Tu, J.; Song, W. L.; Jiao, H.; Xiao, X.; Jiao, S. A Dual-Protection Strategy Using CMK-3 Coated Selenium and Modified Separators for High-Energy Al-Se Batteries. *Inorg. Chem. Front.* **2021**, *8* (4), 1030–1038.
- (82) Zhang, T.; Cai, T.; Xing, W.; Li, T.; Liang, B.; Hu, H.; Zhao, L.; Li, X.; Yan, Z. A Rechargeable 6-Electron Al-Se Battery with High Energy Density. *Energy Storage Mater.* **2021**, *41*, 667–676.
- (83) Li, G.; Kou, M.; Tu, J.; Luo, Y.; Wang, M.; Jiao, S. Coordination Interaction Boosts Energy Storage in Rechargeable Al Battery with a Positive Electrode Material of CuSe. *Chem. Eng. J.* **2021**, *421*, 127792.
- (84) Li, J.; Liu, W.; Yu, Z.; Deng, J.; Zhong, S.; Xiao, Q.; Chen, F.; Yan, D. N-Doped C@ZnSe as a Low Cost Positive Electrode for Aluminum-Ion Batteries: Better Electrochemical Performance with High Voltage Platform of ~ 1.8 V and New Reaction Mechanism. *Electrochim. Acta* **2021**, *370*, 137790.
- (85) Zhang, Y.; Zhang, B.; Li, J.; Liu, J.; Huo, X.; Kang, F. SnSe Nano-Particles as Advanced Positive Electrode Materials for Rechargeable Aluminum-Ion Batteries. *Chem. Eng. J.* **2021**, *403*, 126377.
- (86) Liu, S.; Zhang, X.; He, S.; Tang, Y.; Wang, J.; Wang, B.; Zhao, S.; Su, H.; Ren, Y.; Zhang, L.; Huang, J.; Yu, H.; Amine, K. An Advanced High Energy-Efficiency Rechargeable Aluminum-Selenium Battery. *Nano Energy* **2019**, *66*, 104159.
- (87) Chen, Z.; Mo, F.; Wang, T.; Yang, Q.; Huang, Z.; Wang, D.; Liang, G.; Chen, A.; Li, Q.; Guo, Y.; Li, X.; Fan, J.; Zhi, C. Zinc/Selenium Conversion Battery: A System Highly Compatible with Both Organic and Aqueous Electrolytes. *Energy Environ. Sci.* **2021**, *14* (4), 2441–2450.
- (88) Zhou, R.; Hou, Z.; Liu, Q.; Du, X.; Huang, J.; Zhang, B. Unlocking the Reversible Selenium Electrode for Non-Aqueous and Aqueous Calcium-Ion Batteries. *Adv. Funct. Mater.* **2022**, *32* (26), 220929.
- (89) Wei, Y.; Tao, Y.; Kong, Z.; Liu, L.; Wang, J.; Qiao, W.; Ling, L.; Long, D. Unique Electrochemical Behavior of Heterocyclic Selenium-Sulfur Cathode Materials in Ether-Based Electrolytes for Rechargeable Lithium Batteries. *Energy Storage Mater.* **2016**, *5*, 171–179.
- (90) He, J.; Lv, W.; Chen, Y.; Xiong, J.; Wen, K.; Xu, C.; Zhang, W.; Li, Y.; Qin, W.; He, W. Direct Impregnation of Se₂ into a MOF-Derived 3D Nanoporous Co-N-C Architecture towards Superior Rechargeable Lithium Batteries. *J. Mater. Chem. A Mater.* **2018**, *6* (22), 10466–10473.

- (91) Pham, V. H.; Boscoboinik, J. A.; Stacchiola, D. J.; Self, E. C.; Manikandan, P.; Nagarajan, S.; Wang, Y.; Pol, V. G.; Nanda, J.; Paek, E.; Mitlin, D. Selenium-Sulfur (SeS) Fast Charging Cathode for Sodium and Lithium Metal Batteries. *Energy Storage Mater.* **2019**, *20*, 71–79.
- (92) Xu, G. L.; Sun, H.; Luo, C.; Estevez, L.; Zhuang, M.; Gao, H.; Amine, R.; Wang, H.; Zhang, X.; Sun, C. J.; Liu, Y.; Ren, Y.; Heald, S. M.; Wang, C.; Chen, Z.; Amine, K. Solid-State Lithium/Selenium-Sulfur Chemistry Enabled via a Robust Solid-Electrolyte Interphase. *Adv. Energy Mater.* **2019**, *9* (2), 1802235.
- (93) Meng, T.; Liu, Y.; Li, L.; Zhu, J.; Gao, J.; Zhang, H.; Ma, L.; Li, C. M.; Jiang, J. Smart Merit Combination of Sulfur, Selenium and Electrode Engineering to Build Better Sustainable Li-Storage Batteries. *ACS Sustain. Chem. Eng.* **2019**, *7* (1), 802–809.
- (94) Gu, X.; Tang, T.; Liu, X.; Hou, Y. Rechargeable Metal Batteries Based on Selenium Cathodes: Progress, Challenges and Perspectives. *J. Mater. Chem. A* **2019**, *7*, 11566–11583.
- (95) Shen, C.; Wang, T.; Xu, X.; Tian, X. 3D Printed Cellular Cathodes with Hierarchical Pores and High Mass Loading for Li-SeS₂ Battery. *Electrochim. Acta* **2020**, *349*, 136331.
- (96) Hu, J.; Ren, Y.; Zhang, L. Dual-Confined SeS₂ Cathode Based on Polyaniline-Assisted Double-Layered Micro/Mesoporous Carbon Spheres for Advanced Li-SeS₂ Battery. *J. Power Sources* **2020**, *455*, 227955.
- (97) Lin, S.; Chen, Y.; Wang, Y.; Cai, Z.; Xiao, J.; Muhmood, T.; Hu, X. Three-Dimensional Ordered Porous Nanostructures for Lithium-Selenium Battery Cathodes That Confer Superior Energy-Storage Performance. *ACS Appl. Mater. Interfaces* **2021**, *13* (8), 9955–9964.
- (98) Zhang, Y.; Wang, M.; Guo, Y.; Huang, L.; Wang, B.; Wei, Y.; Jing, P.; Zhang, Y.; Zhang, Y.; Wang, Q.; Sun, J.; Wu, H. A Natural Polymer Captor for Immobilizing Polysulfide/Polyselenide in Working Li-SeS₂ Batteries. *Nanomicro Lett.* **2021**, *13* (1), 104.
- (99) Huang, Y.; Wang, Z.; Guan, M.; Wu, F.; Chen, R. Toward Rapid-Charging Sodium-Ion Batteries Using Hybrid-Phase Molybdenum Sulfide Selenide-Based Anodes. *Adv. Mater.* **2020**, *32* (40), 2003534.
- (100) Du, A.; Zhao, Y.; Zhang, Z.; Dong, S.; Cui, Z.; Tang, K.; Lu, C.; Han, P.; Zhou, X.; Cui, G. Selenium Sulfide Cathode with Copper Foam Interlayer for Promising Magnesium Electrochemistry. *Energy Storage Mater.* **2020**, *26*, 23–31.
- (101) Bai, Y.; Zhang, H.; Song, H.; Zhu, C.; Yan, L.; Hu, Q.; Li, C. M. Engineering Anion Defects of Ternary V-S-Se Layered Cathodes for Ultrafast Zinc Ion Storage. *Nano Energy* **2024**, *120*, 109090.
- (102) Kim, H.; Choi, H. N.; Kim, M. J.; Kansara, S.; Kim, J. T.; Shin, M. S.; Hwang, J. Y.; Jung, H. G.; Ming, J.; Sun, Y. K. Hierarchical Nanowire Host Material for High-Areal-Capacity All-Solid-State S/SeS₂ Batteries. *Adv. Funct. Mater.* **2025**, *35*, 2415299.
- (103) Zhang, Z.; Jiang, S.; Lai, Y.; Li, J.; Song, J.; Li, J. Selenium Sulfide@mesoporous Carbon Aerogel Composite for Rechargeable Lithium Batteries with Good Electrochemical Performance. *J. Power Sources* **2015**, *284*, 95–102.
- (104) Li, Z.; Zhang, J.; Wu, H. B.; Lou, X. W. D. An Improved Li-SeS₂ Battery with High Energy Density and Long Cycle Life. *Adv. Energy Mater.* **2017**, *7* (15), 1700281.
- (105) Zhang, J.; Li, Z.; Lou, X. W. A Freestanding Selenium Disulfide Cathode Based on Cobalt Disulfide-Decorated Multichannel Carbon Fibers with Enhanced Lithium Storage Performance. *Angew. Chem. Int. Ed.* **2017**, *129* (45), 14295–14300.
- (106) Wang, J.; Chen, J. H.; Chen, Z. C.; Wu, Z. Y.; Zhong, X. N.; Ke, J. P. The LiTFSI/COFs Fiber as Separator Coating with Bifunction of Inhibition of Lithium Dendrite and Shuttle Effect for Li-SeS₂ Battery. *Coatings* **2022**, *12* (2), 289.
- (107) Li, X.; Li, X.; Liang, J.; Wang, C.; Luo, J.; Li, R.; Sun, X. High-Performance All-Solid-State Li-Se Batteries Induced by Sulfide Electrolytes. *Energy Environ. Sci.* **2018**, *11* (10), 2828–2832.
- (108) Xu, Q.-T.; Xue, H.-G.; Guo, S.-P. Status and Prospects of Se_xS_y Cathodes for Lithium/Sodium Storage. *Inorg. Chem. Front.* **2019**, *6* (6), 1326–1340.
- (109) Peng, X.; Wang, L.; Zhang, X.; Gao, B.; Fu, J.; Xiao, S.; Huo, K.; Chu, P. K. Reduced Graphene Oxide Encapsulated Selenium Nanoparticles for High-Power Lithium-Selenium Battery Cathode. *J. Power Sources* **2015**, *288*, 214–220.
- (110) Liu, L.; Hou, Y.; Wu, X.; Xiao, S.; Chang, Z.; Yang, Y.; Wu, Y. Nanoporous Selenium as a Cathode Material for Rechargeable Lithium-Selenium Batteries. *Chem. Commun.* **2013**, *49* (98), 11515–11517.
- (111) Wang, M.; Xia, X.; Zhong, Y.; Wu, J.; Xu, R.; Yao, Z.; Wang, D.; Tang, W.; Wang, X.; Tu, J. Porous Carbon Hosts for Lithium-Sulfur Batteries. *Chem.—Eur. J.* **2019**, *25* (15), 3710–3725.
- (112) Jin, J.; Tian, X.; Srikanth, N.; Kong, L. B.; Zhou, K. Advances and Challenges of Nanostructured Electrodes for Li-Se Batteries. *J. Mater. Chem. A* **2017**, *5* (21), 10110–10126.
- (113) Liu, Y.; Si, L.; Zhou, X.; Liu, X.; Xu, Y.; Bao, J.; Dai, Z. A Selenium-Confined Microporous Carbon Cathode for Ultrastable Lithium-Selenium Batteries. *J. Mater. Chem. A* **2014**, *2* (42), 17735–17739.
- (114) Liu, Y.; Si, L.; Du, Y.; Zhou, X.; Dai, Z.; Bao, J. Strongly Bonded Selenium/Microporous Carbon Nanofibers Composite as a High-Performance Cathode for Lithium-Selenium Batteries. *J. Phys. Chem. C* **2015**, *119* (49), 27316–27321.
- (115) Zhou, J.; Yang, J.; Xu, Z.; Zhang, T.; Chen, Z.; Wang, J. A High Performance Lithium-Selenium Battery Using a Microporous Carbon Confined Selenium Cathode and a Compatible Electrolyte. *J. Mater. Chem. A* **2017**, *5* (19), 9350–9357.
- (116) Zhang, H.; Jia, D.; Yang, Z.; Yu, F.; Su, Y.; Wang, D.; Shen, Q. Alkaline Lignin Derived Porous Carbon as an Efficient Scaffold for Lithium-Selenium Battery Cathode. *Carbon* **2017**, *122*, 547–555.
- (117) Guo, B.; Mi, H.; Zhang, P.; Ren, X.; Li, Y. Free-Standing Selenium Impregnated Carbonized Leaf Cathodes for High-Performance Sodium-Selenium Batteries. *Nanoscale Res. Lett.* **2019**, *14*, 30.
- (118) Zeng, L.; Wei, X.; Wang, J.; Jiang, Y.; Li, W.; Yu, Y. Flexible One-Dimensional Carbon-Selenium Composite Nanofibers with Superior Electrochemical Performance for Li-Se/Na-Se Batteries. *J. Power Sources* **2015**, *281*, 461–469.
- (119) Lai, Y.; Gan, Y.; Zhang, Z.; Chen, W.; Li, J. Metal-Organic Frameworks-Derived Mesoporous Carbon for High Performance Lithium-Selenium Battery. *Electrochim. Acta* **2014**, *146*, 134–141.
- (120) Han, K.; Liu, Z.; Shen, J.; Lin, Y.; Dai, F.; Ye, H. A Free-Standing and Ultralong-Life Lithium-Selenium Battery Cathode Enabled by 3D Mesoporous Carbon/Graphene Hierarchical Architecture. *Adv. Funct. Mater.* **2015**, *25* (3), 455–463.
- (121) He, J.; Chen, Y.; Lv, W.; Wen, K.; Li, P.; Wang, Z.; Zhang, W.; Qin, W.; He, W. Three-Dimensional Hierarchical Graphene-CNT@Se: A Highly Efficient Freestanding Cathode for Li-Se Batteries. *ACS Energy Lett.* **2016**, *1* (1), 16–20.
- (122) Yang, C. P.; Xin, S.; Yin, Y. X.; Ye, H.; Zhang, J.; Guo, Y. G. An Advanced Selenium-Carbon Cathode for Rechargeable Lithium-Selenium Batteries. *Angew. Chem. Int. Ed.* **2013**, *52* (32), 8363–8367.
- (123) Ding, J.; Zhou, H.; Zhang, H.; Tong, L.; Mitlin, D. Selenium Impregnated Monolithic Carbons as Free-Standing Cathodes for High Volumetric Energy Lithium and Sodium Metal Batteries. *Adv. Energy Mater.* **2018**, *8* (8), 1701918.
- (124) Wang, H.; Jiang, Y.; Manthiram, A. Long Cycle Life, Low Self-Discharge Sodium-Selenium Batteries with High Selenium Loading and Suppressed Polyselenide Shuttling. *Adv. Energy Mater.* **2018**, *8* (7), 1–8.
- (125) Mukkabl, R.; Deshagani, S.; Meduri, P.; Deepa, M.; Ghosal, P. Selenium/Graphite Platelet Nanofiber Composite for Durable Li-Se Batteries. *ACS Energy Lett.* **2017**, *2* (6), 1288–1295.
- (126) Dong, W. D.; Wang, C. Y.; Li, C. F.; Xia, F. J.; Yu, W. B.; Wu, L.; Mohamed, H. S. H.; Hu, Z. Y.; Liu, J.; Chen, L. H.; Li, Y.; Su, B. L. The Free-Standing N-Doped Murray Carbon Framework with the Engineered Quasi-Optimal Se/C Interface for High-Se-Loading Li/Na-Se Batteries at Elevated Temperature. *Mater. Today Energy* **2021**, *21*, 100808.

- (127) Zhao, D.; Wang, L.; Qiu, M.; Zhang, N. Amorphous Se Restrained by Biomass-Derived Defective Carbon for Stable Na-Se Batteries. *ACS Appl. Energy Mater.* **2021**, *4* (7), 7219–7225.
- (128) Rashad, M.; Asif, M. Recycling Biowaste to Synthesize Nitrogen-Doped Highly Porous Activated Carbon Scaffolds for Selenium Stuffing with Superior Electrochemical Properties. *ACS Appl. Energy Mater.* **2021**, *4* (3), 2786–2796.
- (129) Zhao, X.; Yin, L.; Zhang, T.; Zhang, M.; Fang, Z.; Wang, C.; Wei, Y.; Chen, G.; Zhang, D.; Sun, Z.; Li, F. Heteroatoms Dual-Doped Hierarchical Porous Carbon-Selenium Composite for Durable Li-Se and Na-Se Batteries. *Nano Energy* **2018**, *49*, 137–146.
- (130) Hong, Y. J.; Kang, Y. C. Selenium-Impregnated Hollow Carbon Microspheres as Efficient Cathode Materials for Lithium-Selenium Batteries. *Carbon* **2017**, *111*, 198–206.
- (131) Jayan, R.; Islam, M. M. Functionalized MXenes as Effective Polyselenide Immobilizers for Lithium-Selenium Batteries: A Density Functional Theory (DFT) Study. *Nanoscale* **2020**, *12* (26), 14087–14095.
- (132) Feng, J.; Yu, S.; Shi, C.; Tang, X.; Zhao, X.; Chen, S.; Song, J. Advanced Cathode Designs for High-Energy Lithium/Sodium-Selenium Battery. *Adv. Funct. Mater.* **2025**, DOI: 10.1002/adfm.202422013.
- (133) Lu, P.; Liu, F.; Zhou, F.; Qin, J.; Shi, H.; Wu, Z. S. Lignin Derived Hierarchical Porous Carbon with Extremely Suppressed Polyselenide Shuttling for High-Capacity and Long-Cycle-Life Lithium-Selenium Batteries. *J. Energy Chem.* **2021**, *55*, 476–483.
- (134) Zhao, X.; Yin, L.; Yang, Z.; Chen, G.; Yue, H.; Zhang, D.; Sun, Z.; Li, F. An Alkali Metal-Selenium Battery with a Wide Temperature Range and Low Self-Discharge. *J. Mater. Chem. A* **2019**, *7* (38), 21774–21782.
- (135) Li, J.; Song, J.; Luo, L.; Zhang, H.; Feng, J.; Zhao, X.; Guo, X.; Dong, H.; Chen, S.; Liu, H.; Shao, G.; Anthopoulos, T. D.; Su, Y.; Wang, F.; Wang, G. Synergy of MXene with Se Infiltrated Porous N-Doped Carbon Nanofibers as Janus Electrodes for High-Performance Sodium/Lithium-Selenium Batteries. *Adv. Energy Mater.* **2022**, *12* (32), 2200894.
- (136) Zhang, J.; He, H.; Liu, L.; Wang, G.; Chen, J.; Hu, Z.; Hu, X. Built-in Electric Field by CoSe₂-CoS₂ Mott Schottk Heterostructure: Promoting Rapid Conversion and Ordered Deposition of Polyselenides in Lithium Selenium Batteries. *Chem. Eng. J.* **2024**, *483*, 149401.
- (137) Qu, Y.; Zhang, Z.; Jiang, S.; Wang, X.; Lai, Y.; Liu, Y.; Li, J. Confining Selenium in Nitrogen-Containing Hierarchical Porous Carbon for High-Rate Rechargeable Lithium-Selenium Batteries. *J. Mater. Chem. A* **2014**, *2* (31), 12255–12261.
- (138) Kalimuthu, B.; Nallathamby, K. Designed Formulation of Se-Impregnated N-Containing Hollow Core Mesoporous Shell Carbon Spheres: Multifunctional Potential Cathode for Li-Se and Na-Se Batteries. *ACS Appl. Mater. Interfaces* **2017**, *9* (32), 26756–26770.
- (139) Ren, J.; Huang, Y.; Zhu, H.; Zhang, B.; Zhu, H.; Shen, S.; Tan, G.; Wu, F.; He, H.; Lan, S.; Xia, X.; Liu, Q. Recent Progress on MOF-Derived Carbon Materials for Energy Storage. *Carbon Energy* **2020**, *2*, 176–202.
- (140) Peng, Y.; Xu, J.; Xu, J.; Ma, J.; Bai, Y.; Cao, S.; Zhang, S.; Pang, H. Metal-Organic Framework (MOF) Composites as Promising Materials for Energy Storage Applications. *Adv. Colloid Interface Sci.* **2022**, *307*, 102732.
- (141) Xu, Q.; Liu, H.; Du, W.; Zhan, R.; Hu, L.; Bao, S.; Dai, C.; Liu, F.; Xu, M. Metal-Organic Complex Derived Hierarchical Porous Carbon as Host Matrix for Rechargeable Na-Se Batteries. *Electrochim. Acta* **2018**, *276*, 21–27.
- (142) Li, S.; Yang, H.; Xu, R.; Jiang, Y.; Gong, Y.; Gu, L.; Yu, Y. Selenium Embedded in MOF-Derived N-Doped Microporous Carbon Polyhedrons as a High Performance Cathode for Sodium-Selenium Batteries. *Mater. Chem. Front.* **2018**, *2* (8), 1574–1582.
- (143) Park, S. K.; Park, J. S.; Kang, Y. C. Metal-Organic-Framework-Derived N-Doped Hierarchically Porous Carbon Polyhedrons Anchored on Crumpled Graphene Balls as Efficient Selenium Hosts for High-Performance Lithium-Selenium Batteries. *ACS Appl. Mater. Interfaces* **2018**, *10* (19), 16531–16540.
- (144) Liu, T.; Jia, M.; Zhang, Y.; Han, J.; Li, Y.; Bao, S. J.; Liu, D.; Jiang, J.; Xu, M. Confined Selenium within Metal-Organic Frameworks Derived Porous Carbon Microcubes as Cathode for Rechargeable Lithium-Selenium Batteries. *J. Power Sources* **2017**, *341*, 53–59.
- (145) He, J.; Lv, W.; Chen, Y.; Xiong, J.; Wen, K.; Xu, C.; Zhang, W.; Li, Y.; Qin, W.; He, W. Three-Dimensional Hierarchical C-Co-N/Se Derived from Metal-Organic Framework as Superior Cathode for Li-Se Batteries. *J. Power Sources* **2017**, *363*, 103–109.
- (146) Park, S. K.; Park, J. S.; Kang, Y. C. Selenium-Infiltrated Metal-Organic Framework-Derived Porous Carbon Nanofibers Comprising Interconnected Bimodal Pores for Li-Se Batteries with High Capacity and Rate Performance. *J. Mater. Chem. A* **2018**, *6* (3), 1028–1036.
- (147) Choi, D. S.; Yeom, M. S.; Kim, Y. T.; Kim, H.; Jung, Y. Polyselenide Anchoring Using Transition-Metal Disulfides for Enhanced Lithium-Selenium Batteries. *Inorg. Chem.* **2018**, *57* (4), 2149–2156.
- (148) Zhang, F.; Xiong, P.; Guo, X.; Zhang, J.; Yang, W.; Wu, W.; Liu, H.; Wang, G. A Nitrogen, Sulphur Dual-Doped Hierarchical Porous Carbon with Interconnected Conductive Polyaniline Coating for High-Performance Sodium-Selenium Batteries. *Energy Storage Mater.* **2019**, *19*, 251–260.
- (149) Zhang, J.; Xu, Y.; Fan, L.; Zhu, Y.; Liang, J.; Qian, Y. Graphene-Encapsulated Selenium/Polyaniline Core-Shell Nanowires with Enhanced Electrochemical Performance for Li-Se Batteries. *Nano Energy* **2015**, *13*, 592–600.
- (150) Ma, D.; Li, Y.; Yang, J.; Mi, H.; Luo, S.; Deng, L.; Yan, C.; Zhang, P.; Lin, Z.; Ren, X.; Li, J.; Zhang, H. Atomic Layer Deposition-Enabled Ultrastable Freestanding Carbon-Selenium Cathodes with High Mass Loading for Sodium-Selenium Battery. *Nano Energy* **2018**, *43*, 317–325.
- (151) Xiang, H.; Deng, N.; Zhao, H.; Wang, X.; Wei, L.; Wang, M.; Cheng, B.; Kang, W. A Review on Electronically Conducting Polymers for Lithium-Sulfur Battery and Lithium-Selenium Battery: Progress and Prospects. *Journal of Energy Chemistry* **2021**, 523–556, DOI: 10.1016/j.jechem.2020.10.029.
- (152) Guo, J.; Wen, Z.; Ma, G.; Jin, J.; Wang, W.; Liu, Y. A Selenium@polypyrrole Hollow Sphere Cathode for Rechargeable Lithium Batteries. *RSC Adv.* **2015**, *5* (26), 20346–20350.
- (153) Li, Z.; Zhang, J.; Lu, Y.; Lou, X. W. A Pyrolyzed Polyacrylonitrile/Selenium Disulfide Composite Cathode with Remarkable Lithium and Sodium Storage Performances. *Sci. Adv.* **2018**, *4* (6), 1–11.
- (154) Zhang, Z.; Yang, X.; Wang, X.; Li, Q.; Zhang, Z. TiO₂-Se Composites as Cathode Material for Rechargeable Lithium-Selenium Batteries. *Solid State Ion* **2014**, *260*, 101–106.
- (155) Li, X.; Xiang, Y.; Qu, B.; Su, S. A Facial Method to Synthesize Se/NiO Composites for High Performance Lithium Ion Battery Electrodes. *Mater. Lett.* **2017**, *203*, 1–4.
- (156) Zhao, X.; Jiang, L.; Ma, C.; Cheng, L.; Wang, C.; Chen, G.; Yue, H.; Zhang, D. The Synergistic Effects of Nanoporous Fiber TiO₂ and Nickel Foam Interlayer for Ultra-Stable Performance in Lithium-Selenium Batteries. *J. Power Sources* **2021**, *490*, 229534.
- (157) Aboonassar Shiraz, M. H.; Zhu, H.; Liu, J. Nanoscale Al₂O₃ Coating to Stabilize Selenium Cathode for Sodium-Selenium Batteries. *J. Mater. Res.* **2020**, *35* (7), 747–755.
- (158) Dong, S.; Chen, X.; Zhang, X.; Cui, G. Nanostructured Transition Metal Nitrides for Energy Storage and Fuel Cells. *Coord. Chem. Rev.* **2013**, *257*, 1946–1956.
- (159) Lu, T.; Dong, S.; Zhang, C.; Zhang, L.; Cui, G. Fabrication of Transition Metal Selenides and Their Applications in Energy Storage. *Coord. Chem. Rev.* **2017**, 75–99, DOI: 10.1016/j.ccr.2016.11.005.
- (160) Li, D.; Chen, X.; Xiang, P.; Du, H.; Xiao, B. Chalcogenated-Ti₃C₂X₂ MXene (X = O, S, Se and Te) as a High-Performance Anode Material for Li-Ion Batteries. *Appl. Surf. Sci.* **2020**, *501*, 144221.
- (161) Li, J.; Kong, Z.; Liu, X.; Zheng, B.; Fan, Q. H.; Garratt, E.; Schuelke, T.; Wang, K.; Xu, H.; Jin, H. Strategies to Anode Protection

- in Lithium Metal Battery: A Review. *InfoMat* **2021**, *3* (12), 1333–1363.
- (162) Lee, J. T.; Kim, H.; Nitta, N.; Eom, K. S.; Lee, D. C.; Wu, F.; Lin, H. T.; Zdyrko, B.; Cho, W. I.; Yushin, G. Stabilization of Selenium Cathodes via in Situ Formation of Protective Solid Electrolyte Layer. *J. Mater. Chem. A Mater.* **2014**, *2* (44), 18898–18905.
- (163) Hasa, I.; Mariyappan, S.; Saurel, D.; Adelhalm, P.; Kopolov, A. Y.; Masquelier, C.; Croguennec, L.; Casas-Cabanas, M. Challenges of Today for Na-Based Batteries of the Future: From Materials to Cell Metrics. *J. Power Sources* **2021**, *482*, 228872.
- (164) Manthiram, A.; Yu, X.; Wang, S. Lithium Battery Chemistries Enabled by Solid-State Electrolytes. *Nature Reviews Materials* **2017**, *16103* DOI: 10.1038/natrevmats.2016.103.
- (165) Lourenço, T. C.; Dias, L. G.; Da Silva, J. L. F. Theoretical Investigation of the Na+Transport Mechanism and the Performance of Ionic Liquid-Based Electrolytes in Sodium-Ion Batteries. *ACS Appl. Energy Mater.* **2021**, *4* (5), 4444–4458.
- (166) Chen, X.; Shen, X.; Hou, T. Z.; Zhang, R.; Peng, H. J.; Zhang, Q. Ion-Solvent Chemistry-Inspired Cation-Additive Strategy to Stabilize Electrolytes for Sodium-Metal Batteries. *Chem.* **2020**, *6* (9), 2242–2256.
- (167) Dong, Y.; Lu, P.; Ding, Y.; Shi, H.; Feng, X.; Wu, Z. Advanced Design of Cathodes and Interlayers for High-performance Lithium-selenium Batteries. *SusMat* **2021**, *1* (3), 393–412.
- (168) Zhang, Q.; Cai, L.; Liu, G.; Li, Q.; Jiang, M.; Yao, X. Selenium-Infused Ordered Mesoporous Carbon for Room-Temperature All-Solid-State Lithium-Selenium Batteries with Ultrastable Cyclability. *ACS Appl. Mater. Interfaces* **2020**, *12* (14), 16541–16547.
- (169) Yao, X.; Liu, D.; Wang, C.; Long, P.; Peng, G.; Hu, Y. S.; Li, H.; Chen, L.; Xu, X. High-Energy All-Solid-State Lithium Batteries with Ultralong Cycle Life. *Nano Lett.* **2016**, *16* (11), 7148–7154.
- (170) Jin, Y.; Liu, K.; Lang, J.; Jiang, X.; Zheng, Z.; Su, Q.; Huang, Z.; Long, Y.; Wang, C. an; Wu, H.; Cui, Y. High-Energy-Density Solid-Electrolyte-Based Liquid Li-S and Li-Se Batteries. *Joule* **2020**, *4* (1), 262–274.
- (171) Lou, S.; Zhang, F.; Fu, C.; Chen, M.; Ma, Y.; Yin, G.; Wang, J. Interface Issues and Challenges in All-Solid-State Batteries: Lithium, Sodium, and Beyond. *Adv. Mater.* **2021**, *33*, 2000721.
- (172) Zhao, W.; Yi, J.; He, P.; Zhou, H. Solid-State Electrolytes for Lithium-Ion Batteries: Fundamentals, Challenges and Perspectives. *Electrochem. Energy R.* **2019**, *2*, 574–605.
- (173) Xu, R.; Cheng, X. B.; Yan, C.; Zhang, X. Q.; Xiao, Y.; Zhao, C. Z.; Huang, J. Q.; Zhang, Q. Artificial Interphases for Highly Stable Lithium Metal Anode. *Matter* **2019**, *1* (2), 317–344.
- (174) Zhou, D.; Shanmukaraj, D.; Tkacheva, A.; Armand, M.; Wang, G. Polymer Electrolytes for Lithium-Based Batteries: Advances and Prospects. *Chem.* **2019**, *5* (9), 2326–2352.
- (175) Xian, C.; Wang, Q.; Xia, Y.; Cao, F.; Shen, S.; Zhang, Y.; Chen, M.; Zhong, Y.; Zhang, J.; He, X.; Xia, X.; Zhang, W.; Tu, J. Solid-State Electrolytes in Lithium-Sulfur Batteries: Latest Progresses and Prospects. *Small* **2023**, *19*, 2208164.
- (176) Banerjee, A.; Wang, X.; Fang, C.; Wu, E. A.; Meng, Y. S. Interfaces and Interphases in All-Solid-State Batteries with Inorganic Solid Electrolytes. *Chem. R.* **2020**, *120* (14), 6878–6933.
- (177) Zhang, Z.; Shao, Y.; Lotsch, B.; Hu, Y. S.; Li, H.; Janek, J.; Nazar, L. F.; Nan, C. W.; Maier, J.; Armand, M.; Chen, L. New Horizons for Inorganic Solid State Ion Conductors. *Energy Environ. Sci.* **2018**, *11*, 1945–1976.
- (178) Han, X.; Gong, Y.; Fu, K.; He, X.; Hitz, G. T.; Dai, J.; Pearse, A.; Liu, B.; Wang, H.; Rubloff, G.; Mo, Y.; Thangadurai, V.; Wachsman, E. D.; Hu, L. Negating Interfacial Impedance in Garnet-Based Solid-State Li Metal Batteries. *Nat. Mater.* **2017**, *16* (5), 572–579.
- (179) Hong, T. H.; Kim, J. D.; Lee, J. S.; Choi, Y.; Jung, H. Y.; Lee, Y. H.; Hwang, S. Y.; Eom, K. S.; Lee, J. T. Integration of a Composite Polymer Electrolyte and Se/C Cathodes toward High-Performance All-Solidstate Li-Se Batteries. *J. Mater. Chem. A* **2024**, *12* (4), 1998–2003.
- (180) Jiang, C.; Li, H.; Wang, C. Recent Progress in Solid-State Electrolytes for Alkali-Ion Batteries. *Science Bulletin* **2017**, *62* (21), 1473–1490.
- (181) Liu, Y.; Yang, D.; Wang, W.; Hu, K.; Huang, Q.; Zhang, Y.; Miao, Y.; Fu, L.; Wu, M.; Wu, Y. Toward Heat-Tolerant Potassium Batteries Based on Pyrolyzed Selenium Disulfide/Polyacrylonitrile Positive Electrode and Gel Polymer Electrolyte. *J. Mater. Chem. A* **2020**, *8* (8), 4544–4551.
- (182) Manthiram, A.; Fu, Y.; Chung, S. H.; Zu, C.; Su, Y. S. Rechargeable Lithium-Sulfur Batteries. *Chem. R.* **2014**, *114* (23), 11751–11787.
- (183) Goodenough, J. B.; Singh, P. Review—Solid Electrolytes in Rechargeable Electrochemical Cells. *J. Electrochem. Soc.* **2015**, *162* (14), A2387–A2392.
- (184) Lee, J. T.; Kim, H.; Oschatz, M.; Lee, D. C.; Wu, F.; Lin, H. T.; Zdyrko, B.; Il Cho, W.; Kaskel, S.; Yushin, G. Micro- and Mesoporous Carbide-Derived Carbon-Selenium Cathodes for High-Performance Lithium Selenium Batteries. *Adv. Energy Mater.* **2015**, *5* (1), 1400981.
- (185) Aboonassr Shiraz, M. H.; Hu, Y.; Liu, J. A Stable Lithium-Ion Selenium Batteries Enabled by Microporous Carbon/Se and Fluoroethylene Carbonate Additive. *ECS Trans.* **2020**, *97* (7), 279–288.
- (186) Wang, H.; Yu, D.; Kuang, C.; Cheng, L.; Li, W.; Feng, X.; Zhang, Z.; Zhang, X.; Zhang, Y. Alkali Metal Anodes for Rechargeable Batteries. *Chem.* **2019**, *5* (2), 313–338.
- (187) Zhang, Y.; Zuo, T. T.; Popovic, J.; Lim, K.; Yin, Y. X.; Maier, J.; Guo, Y. G. Towards Better Li Metal Anodes: Challenges and Strategies. *Mater. Today* **2020**, *33*, 56–74.
- (188) Cheng, X. B.; Zhang, R.; Zhao, C. Z.; Wei, F.; Zhang, J. G.; Zhang, Q. A Review of Solid Electrolyte Interphases on Lithium Metal Anode. *Adv. Sci.* **2016**, *3* (3), 1500213.
- (189) Tan, J.; Matz, J.; Dong, P.; Shen, J.; Ye, M. A Growing Appreciation for the Role of LiF in the Solid Electrolyte Interphase. *Adv. Energy Mater.* **2021**, *11*, 2100046.
- (190) McBrayer, J. D.; Apblett, C. A.; Harrison, K. L.; Fenton, K. R.; Minteer, S. D. Mechanical Studies of the Solid Electrolyte Interphase on Anodes in Lithium and Lithium Ion Batteries. *Nanotechnology* **2021**, *32* (50), 502005.
- (191) Wang, Z.; Wang, Y.; Wu, C.; Pang, W. K.; Mao, J.; Guo, Z. Constructing Nitrided Interfaces for Stabilizing Li Metal Electrodes in Liquid Electrolytes. *Chem. Sci.* **2021**, *12*, 8945–8966.
- (192) Zhang, C.; Lan, Q.; Liu, Y.; Wu, J.; Shao, H.; Zhan, H.; Yang, Y. A Dual-Layered Artificial Solid Electrolyte Interphase Formed by Controlled Electrochemical Reduction of LiTFSI/DME-LiNO₃ for Dendrite-Free Lithium Metal Anode. *Electrochim. Acta* **2019**, *306*, 407–419.
- (193) Zhang, L.; Ling, M.; Feng, J.; Mai, L.; Liu, G.; Guo, J. The Synergistic Interaction between LiNO₃ and Lithium Polysulfides for Suppressing Shuttle Effect of Lithium-Sulfur Batteries. *Energy Storage Mater.* **2018**, *11*, 24–29.
- (194) Yang, H. W.; Kang, W. S.; Kim, S. J. A Significant Enhancement of Cycling Stability at Fast Charging Rate through Incorporation of Li₃N into LiF-Based SEI in SiO_x Anode for Li-Ion Batteries. *Electrochim. Acta* **2022**, *412*, 140107.
- (195) Zhang, Z.; Wang, J.; Zhang, S.; Ying, H.; Zhuang, Z.; Ma, F.; Huang, P.; Yang, T.; Han, G.; Han, W. Q. Stable All-Solid-State Lithium Metal Batteries with Li₃N-LiF-Enriched Interface Induced by Lithium Nitrate Addition. *Energy Storage Mater.* **2021**, *43*, 229–237.
- (196) Li, C.; Wang, Y.; Li, H.; Liu, J.; Song, J.; Fusaro, L.; Hu, Z. Y.; Chen, Y.; Li, Y.; Su, B. L. Weaving 3D Highly Conductive Hierarchically Interconnected Nanoporous Web by Threading MOF Crystals onto Multi Walled Carbon Nanotubes for High Performance Li-Se Battery. *J. Energy Chem.* **2021**, *59*, 396–404.
- (197) Liu, Y.; He, P.; Zhou, H. Rechargeable Solid-State Li-Air and Li-S Batteries: Materials, Construction, and Challenges. *Adv. Energy Mater.* **2018**, *8*, 1701602.
- (198) Ye, T.; Li, L.; Zhang, Y. Recent Progress in Solid Electrolytes for Energy Storage Devices. *Adv. Funct. Mater.* **2020**, *30*, 2000077.

- (199) Gao, X.; Yang, X.; Wang, S.; Sun, Q.; Zhao, C.; Li, X.; Liang, J.; Zheng, M.; Zhao, Y.; Wang, J.; Li, M.; Li, R.; Sham, T. K.; Sun, X. A 3D-Printed Ultra-High Se Loading Cathode for High Energy Density Quasi-Solid-State Li-Se Batteries. *J. Mater. Chem. A* **2020**, *8* (1), 278–286.
- (200) Guo, J.; Wen, Z.; Wu, M.; Jin, J.; Liu, Y. Vinylene Carbonate-LiNO₃: A Hybrid Additive in Carbonic Ester Electrolytes for SEI Modification on Li Metal Anode. *Electrochem. Commun.* **2015**, *51*, 59–63.
- (201) Shi, P.; Liu, F.; Feng, Y. Z.; Zhou, J.; Rui, X.; Yu, Y. The Synergetic Effect of Lithium Bisoxalatodifluorophosphate and Fluoroethylene Carbonate on Dendrite Suppression for Fast Charging Lithium Metal Batteries. *Small* **2020**, *16* (30), 2001989.
- (202) Fondard, J.; Irisarri, E.; Courrèges, C.; Palacin, M. R.; Ponrouch, A.; Dedryvère, R. SEI Composition on Hard Carbon in Na-Ion Batteries After Long Cycling: Influence of Salts (NaPF₆, NaTFSI) and Additives (FEC, DMCF). *J. Electrochem. Soc.* **2020**, *167* (7), 070526.
- (203) Piao, N.; Liu, S.; Zhang, B.; Ji, X.; Fan, X.; Wang, L.; Wang, P. F.; Jin, T.; Liou, S. C.; Yang, H.; Jiang, J.; Xu, K.; Schroeder, M. A.; He, X.; Wang, C. Lithium Metal Batteries Enabled by Synergetic Additives in Commercial Carbonate Electrolytes. *ACS Energy Lett.* **2021**, *6* (5), 1839–1848.
- (204) Wang, W. P.; Zhang, J.; Li, X. T.; Yin, Y. X.; Xin, S.; Guo, Y. G. Stabilizing the Electrochemistry of Lithium-Selenium Battery via In Situ Gelated Polymer Electrolyte: A Look from Anode. *Chem. Res. Chin. Univ.* **2021**, *37* (2), 298–303.
- (205) Kim, S.; Cho, M.; Lee, Y. High-Performance Li-Se Battery Enabled via a One-Piece Cathode Design. *Adv. Energy Mater.* **2020**, *10* (5), 1903477.
- (206) Gogia, A.; Vallo, N.; Subramanyam, G.; Fellner, J. P.; Kumar, J. Proof-of-Concept Molten Lithium-Selenium Battery. *Energy Fuels* **2021**, *35* (24), 20400–20405.
- (207) Cheng, X.; Pan, J.; Zhao, Y.; Liao, M.; Peng, H. Gel Polymer Electrolytes for Electrochemical Energy Storage. *Adv. Energy Mater.* **2018**, *8*, 1702184.
- (208) Zhu, M.; Wu, J.; Zhong, W. H.; Lan, J.; Sui, G.; Yang, X. A Biobased Composite Gel Polymer Electrolyte with Functions of Lithium Dendrites Suppressing and Manganese Ions Trapping. *Adv. Energy Mater.* **2018**, *8* (11), 1702561.
- (209) Wang, S.; Peng, B.; Lu, J.; Jie, Y.; Li, X.; Pan, Y.; Han, Y.; Cao, R.; Xu, D.; Jiao, S. Recent Progress in Rechargeable Sodium Metal Batteries: A Review. *Chem.—Eur. J.* **2023**, *29*, e202202380.
- (210) Hu, P.; Xiao, F.; Wang, H.; Rogach, A. L. Dual-Functional Hosts Derived from Metal-Organic Frameworks Reduce Dissolution of Polyselenides and Inhibit Dendrite Growth in a Sodium-Selenium Battery. *Energy Storage Mater.* **2022**, *51*, 249–258.
- (211) Dong, P.; Zhang, X.; Cha, Y.; Lee, J. I.; Song, M. K. In Situ Surface Protection of Lithium Metal Anode in Lithium-Selenium Disulfide Batteries with Ionic Liquid-Based Electrolytes. *Nano Energy* **2020**, *69*, 104434.
- (212) Zhu, J.; Li, P.; Chen, X.; Legut, D.; Fan, Y.; Zhang, R.; Lu, Y.; Cheng, X.; Zhang, Q. Rational Design of Graphitic-Inorganic Bi-Layer Artificial SEI for Stable Lithium Metal Anode. *Energy Storage Mater.* **2019**, *16*, 426–433.
- (213) Qi, X.; Jin, Q.; Yang, F.; Jiang, R.; Sun, Q.; Qie, L.; Huang, Y. A Long-Life and Safe Lithiated Graphite-Selenium Cell with Competitive Gravimetric and Volumetric Energy Densities. *J. Energy Chem.* **2021**, *60*, 556–563.
- (214) Albertus, P.; Babinec, S.; Litzelman, S.; Newman, A. Status and Challenges in Enabling the Lithium Metal Electrode for High-Energy and Low-Cost Rechargeable Batteries. *Nat. Energy* **2018**, *3* (1), 16–21.